FUGRO AIRBORNE SURVEYS

Report #2116

LOGISTICS REPORT
HELICOPTER-BORNE
DIGHEM$^{V\text{-}DSP}$ SURVEY
FOR
NORTHGATE EXPLORATION LIMITED
TOODOGGONE AREA
BRITISH COLUMBIA

CROY 1-4 and HEATHER 1-5 MINERAL CLAIMS
OMINECA MINING DIVISION
NTS: 094C05W, 094D08E

LATITUDE: 56° 28' 18"; LONGITUDE: 126° 00' 00"

OWNER/OPERATOR: NORTHGATE EXPLORATION LIMITED

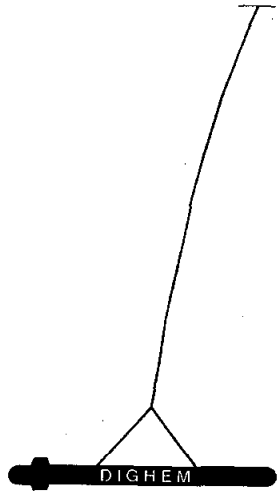

Fugro Airborne Surveys Corp.
Mississauga, Ontario

Mark Stephens, M.Sc.
Geophysicist

October 29, 2002

Fugro Airborne Surveys, 2270 Argentia Road, Unit 2, Mississauga, Ontario, Canada, L5N 6A6
Phone: 1 905 812 0212, Fax: 1 905 812 1504

GEOLOGICAL SURVEY BRANCH
ASSESSMENT REPORT

BRITISH COLUMBIA

Ministry of Energy & Mines
Energy & Minerals Division
Geological Survey Branch

27,238

ASSESSMENT REPORT TITLE PAGE AND SUMMARY

TITLE OF REPORT [type of survey(s)]	TOTAL COST
LOGISTICS REPORT HELICOPTER-BORNE DIGHEM SURVEY	8507.00

AUTHOR(S) MARK STEPHENS MSc SIGNATURE(S)

NOTICE OF WORK PERMIT NUMBER(S)/DATE(S) 10-29-02 YEAR OF WORK 2002

STATEMENT OF WORK - CASH PAYMENT EVENT NUMBER(S)/DATE(S) 3196491

PROPERTY NAME CROY

CLAIM NAME(S) (on which work was done) CROY 1-4, HEATHER 1-5

COMMODITIES SOUGHT Au-Cu-Ag-Mo

MINERAL INVENTORY MINFILE NUMBER(S), IF KNOWN 094D 113

MINING DIVISION OMINECA NTS 94

LATITUDE 56 ° 28 ' 18 " LONGITUDE 126 ° 00 ' 60 " (at centre of work)

OWNER(S)

1) NORTHGATE EXPLORATION LTD 2)

MAILING ADDRESS

PO Box 11179 ROYAL CENTRE
2050-1055 W. GEORGIA ST. VANCOUVER BC V6E 3R5

OPERATOR(S) [who paid for the work]

1) As Above 2)

MAILING ADDRESS

As Above

PROPERTY GEOLOGY KEYWORDS (lithology, age, stratigraphy, structure, alteration, mineralization, size and attitude):

Takla Volcanics, Davie Creek Stock, Alaskan-type Ultramafic.

REFERENCES TO PREVIOUS ASSESSMENT WORK AND ASSESSMENT REPORT NUMBERS 7743, 21521

(OVER)

Executive Summary:

The Croy Property comprised of nine claims (85 units) is located in the Swannell Ranges of north central BC approximately 350km northwest of Prince George at 56°28'N latitude and 126°01'W longitude. The property is accessible via a 15km spur off the Omineca Resource Access Road, or by helicopter from Kemess or Johansen Lake.

The property has been worked intermittently in 1937-38 by Cominco, then by Teck, Chevron and Getty in 1973, 1979, 1981 and 1982, and most recently again by Teck in 1991 and 1992. The most significant work was done on the Davie Creek Molybdenum deposit (100Mt @ 0.10% Mo) which is located on Croy 4.

The Croy Property is underlain by Triassic arc volcanic rocks, and ultramafic intrusive rocks of the Abraham Creek complex. The Triassic rocks are dominantly Takla Formation tuffs and tuffaceous sandstone of andesitic composition. The Abraham Creek complex is an Alaskan-type ultramafic complex comprised of pyroxenite, serpentinite and hornblendite thought to be of late Triassic to early Jurassic age. The Davie Creek Molybdenum deposit is hosted by porphyritic granodiorite, hornblendite, quartz monzonite and altered Takla Group lithologies. These rocks have undergone pervasive potassic alteration with associated chloritic and sericitic alteration. Disseminated chalcopyrite, scheelite, molybdenite and pyrite occur within the stock and hornfelsed rocks.

In 2002, Northgate staked the property as it has potential for Cu-Au and Mo porphyry mineralization and is in close proximity to access and power. The 2002 work program comprised a helicopter-borne high resolution, magnetic and EM airborne geophysical survey completed by Fugro Aerial Surveys. This work was aimed at outlining conductive areas associated with porphyry style alteration, and definition of magnetic anomalies related to intrusive activity. A total of 100 line kilometers at 200m spacing were flown in 2002 on the Croy Property (Croy 1-4 and Heather 1-5 claims).

SUMMARY

This report describes the logistics and results of a DIGHEM$^{V\text{-}DSP}$ airborne geophysical survey carried out for Northgate Exploration Limited, over four properties located in the Toodoggone Area, British Columbia. Total coverage of the survey block amounted to 1824.4 km. The survey was flown from August 12 to August 18, 2002.

The purpose of the survey was to detect zones of conductive mineralization and to provide information which could be used to map the geology and structure of the survey area. This was accomplished by using a DIGHEM$^{V\text{-}DSP}$ multi-coil, multi-frequency electromagnetic system, supplemented by a high sensitivity cesium magnetometer. The information from these sensors was processed to produce maps which display the magnetic, radiometric and conductive properties of the survey areas. A GPS electronic navigation system, utilizing a satellite (UHF) link, ensured accurate positioning of the geophysical data with respect to the base maps. Visual flight path recovery techniques were used to confirm the location of the helicopter where visible topographic features could be identified on the ground.

The survey properties contain several anomalous features, some of which are considered to be of moderate to high priority as exploration targets. Most of the inferred bedrock conductors appear to warrant further investigation using appropriate surface exploration techniques. Areas of interest may be assigned priorities on the basis of supporting geophysical, geochemical and/or geological information. After initial investigations have

been carried out, it may be necessary to re-evaluate the remaining anomalies based on information acquired from the follow-up program.

CONTENTS

APPENDICES

A. List of Personnel
B. Statement of Cost
C. Background Information
D. EM Anomaly List

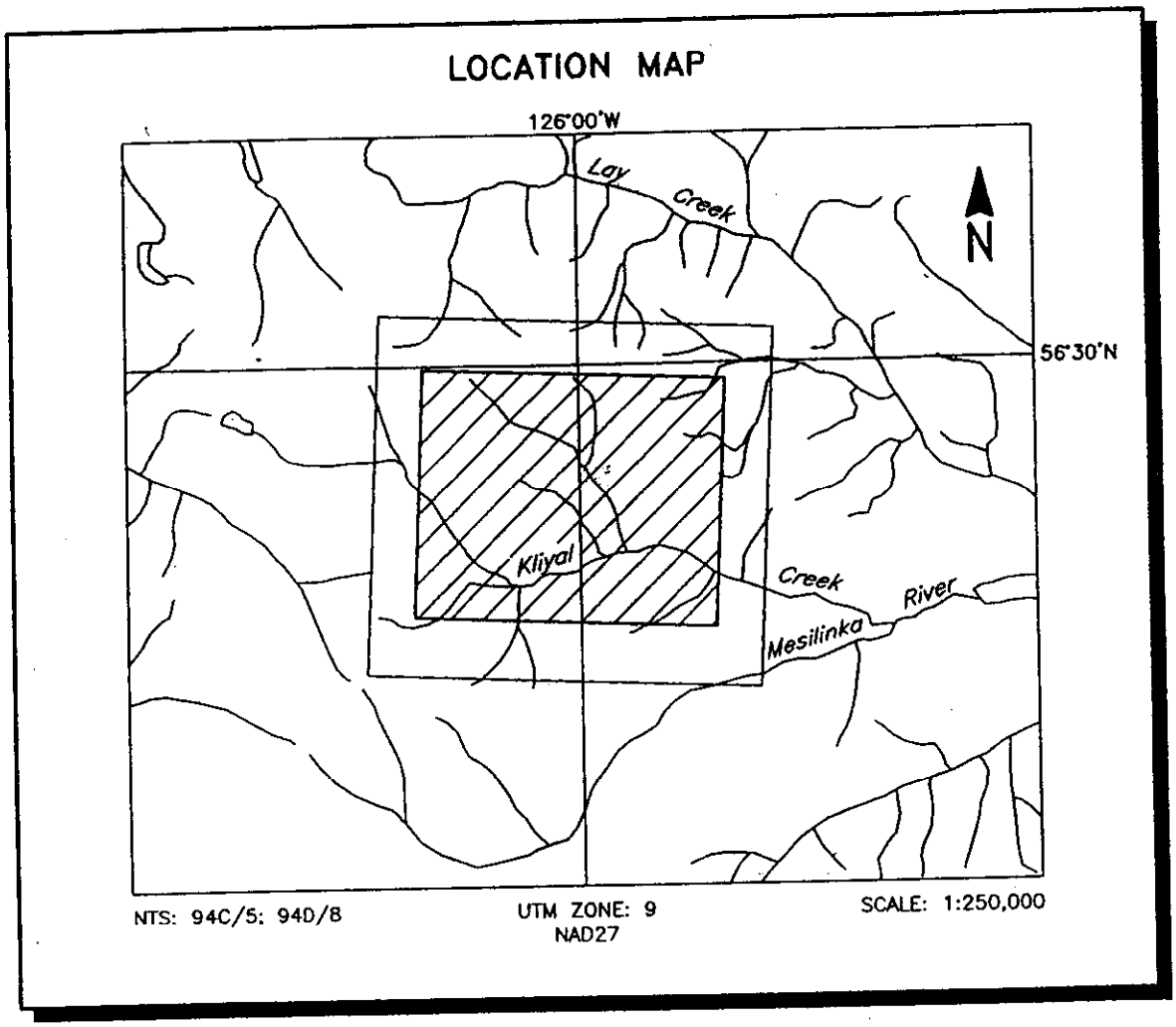

Figure 4
Northgate Exploration Limited
Croy Property, Kliyul Ck.
B.C.
Job#2116

1. INTRODUCTION

A DIGHEM$^{V\text{-}DSP}$ electromagnetic/resistivity/magnetic/radiometric survey was flown for Northgate Exploration Limited, from August 12 to August 18, 2002, over four survey blocks located in the Toodoggone Area, British Columbia. The survey areas can be located on NTS map sheets 94C/5; 94D/8,15,16; 94E/2,7 (Figures 1, 2, 3 and 4).

Survey coverage consisted of approximately 1824 line-km, including tie lines. Flight lines were flown in an azimuthal direction of 90° with a line separation of either 100 or 200 metres. Table 1-1 illustrates the details of each area.

Table 1-1

Area	Flight Line Direction	Flight Line Separation (metres)	Km Flown
Brenda Property	90°	200	287.9
Kemess Mine Property	90°	100	805.8
KG Property	90°	200	283.8
Croy Property	90°	200	446.9

The survey employed the DIGHEM$^{V\text{-}DSP}$ electromagnetic system. Ancillary equipment consisted of a magnetometer, radar and barometric altimeter, video camera, analog and digital recorders, a 512-channel spectrometer and an electronic navigation system. The instrumentation was installed in an AS350B2 turbine helicopter (Registration C-FZTA) which was provided by Questral Helicopters Ltd. The helicopter flew at an average

airspeed of 82 km/h with an EM sensor height of approximately 30 metres. The spectrometer crystal package was housed within the helicopter, with a nominal terrain clearance of 60 metres.

Section 2 provides details on the survey equipment, the data channels, their respective sensitivities, and the navigation/flight path recovery procedure. Noise levels of less than 2 ppm are generally maintained for wind speeds up to 35 km/h. Higher winds may cause the system to be grounded because excessive bird swinging produces difficulties in flying the helicopter. The swinging results from the 5 m^2 of area which is presented by the bird to broadside gusts.

In some portions of the survey area, the steep topography forced the pilot to exceed normal terrain clearance for reasons of safety. It is possible that some weak conductors may have escaped detection in areas where the bird height exceeded 120 m. In difficult areas where near-vertical climbs were necessary, the forward speed of the helicopter was reduced to a level which permitted excessive bird swinging. This problem, combined with the severe stresses to which the bird was subjected, gave rise to aerodynamic noise levels which are slightly higher than normal on some lines. Where warranted, reflights were carried out to minimize these adverse effects.

Due to the presence of cultural features in the survey areas, any interpreted conductors which occur in close proximity to cultural sources, should be confirmed as bedrock conductors prior to drilling.

2. SURVEY EQUIPMENT

This section provides a brief description of the geophysical instruments used to acquire the survey data and the calibration procedures employed.

Electromagnetic System

Model: DIGHEM$^{V\text{-}DSP}$

Type: Towed bird, symmetric dipole configuration operated at a nominal survey altitude of 30 metres. Coil separation is 8 metres for 900 Hz, 1000 Hz, 5500 Hz and 7200 Hz, and 6.3 metres for the 56,000 Hz coil-pair.

Coil orientations/frequencies:

orientation		nominal	actual
coaxial	/	1000 Hz	1058 Hz
coplanar	/	900 Hz	866 Hz
coaxial	/	5500 Hz	5722 Hz
coplanar	/	7200 Hz	7235 Hz
coplanar	/	56,000 Hz	55,603 Hz

Channels recorded:
5 in-phase channels
5 quadrature channels
2 monitor channels

Sensitivity:

0.06 ppm at	1000 Hz Cx
0.12 ppm at	900 Hz Cp
0.12 ppm at	5500 Hz Cx
0.24 ppm at	7200 Hz Cp
0.60 ppm at	56,000 Hz Cp

Sample rate: 10 per second, equivalent to 1 sample every 3 m, at a survey speed of 110 km/h.

The electromagnetic system utilizes a multi-coil coaxial/coplanar technique to energize conductors in different directions. The coaxial coils are vertical with their axes in the flight direction. The coplanar coils are horizontal. The secondary fields are sensed simultaneously by means of receiver coils which are maximum coupled to their respective transmitter coils. The system yields an in-phase and a quadrature channel from each transmitter-receiver coil-pair.

DSP System Calibration

The phase calibration adjusts the phase angle of the receiver to match that of the transmitter. The initial phase calibration is conducted with a ferrite bar on the ground, and subsequent calibrations are conducted in the air using a calibration coil in the bird. A ferrite bar, which produces a purely in-phase anomaly, is positioned near each receiver coil. The bar is rotated from minimum to maximum field coupling and the responses for the in-phase and quadrature components for each coil-pair/frequency are measured. The phase of the response is adjusted at the console to return an in-phase only response for each coil-pair. Phase checks are performed daily.

The ferrite bar phase calibrations measure a relative change in the secondary field, rather than an absolute value. This removes any dependency of the calibration procedure on the secondary field due to the ground, except under circumstances of extreme ground conductivity

Calibrations of the gain, phase and the system zero level are performed in the air, before, after, and at regular intervals during each flight. The system is flown to an altitude high enough to be out of range of any secondary field from the earth (the altitude is dependent on ground resistivity) at which point the zero, or base level of the system is measured. Calibration coils in the bird are activated for each frequency in turn by closing a switch to form a closed circuit through the coil. The transmitter induces a current in this loop, which creates a secondary field in the receiver of precisely known phase and amplitude. The phase and gain of the system are automatically adjusted by the digital receiver to set the measured calibration signal to the known values for the system.

Magnetometer

Model:	Fugro AM102 processor with a Scintrex CS2 sensor
Type:	Optically pumped cesium vapour
Sensitivity:	0.01 nT
Sample rate:	10 per second

The magnetometer sensor is housed in the EM bird, 30 m below the helicopter.

Magnetic Base Station

Model: Fugro CF1 base station

Sensor type: Geometrics G823A sensor

Counter specifications:
- Accuracy: ±0.1 nT
- Resolution: 0.01 nT
- Sample rate 1 Hz

GPS specifications:
- Model: Marconi Allstar
- Accuracy of time-base with respect to UTC: 0.25 seconds
- Sample rate: 1 Hz

Environmental Monitor specifications:

Temperature:
- Accuracy: ±1.5°C max
- Resolution: 0.0305°C
- Sample rate: 1 Hz
- Range: -40°C to +75°C

Barometric pressure:
- Model: Motorola MPXA4115A
- Accuracy: ±3.0° kPa max (-20°C to 105°C temp. ranges)
- Resolution: 0.013 kPa
- Sample rate: 1 Hz
- Range: 55 kPa to 108 kPa

Back-up

Model: GEM Systems GSM-19T

Type: Digital recording proton precession

Sensitivity: 0.10 nT

Sample rate: 0.2 per second

A digital recorder is operated in conjunction with the base station magnetometer to record the diurnal variations of the earth's magnetic field. The clock of the base station is synchronized with that of the airborne system to permit subsequent removal of diurnal drift.

Spectrometer

Manufacturer:	Exploranium
Model:	GR-820
Type:	512 Multichannel, Potassium stabilized
Accuracy:	1 count/sec.
Update:	1 integrated sample/sec.

The GR-820 Airborne Spectrometer employs four downward looking crystals (1024 cu.in.) and one upward looking crystal (256 cu.in.). The downward crystal records the radiometric spectrum from 410 KeV to 3 MeV over 256 discrete energy windows, as well as a cosmic ray channel which detects photons with energy levels above 3.0 MeV. From these 256 channels, the standard Total Count, Potassium, Uranium and Thorium channels are extracted. The upward crystal is used to measure and correct for Radon.

The shock-protected Sodium Iodide (Thallium) crystal package is unheated, and is automatically stabilized with respect to the Potassium peak. The GR-820 provides raw or

Compton stripped data which has been automatically corrected for gain, base level, ADC offset and dead time.

The system is calibration before and after each flight using three accurately positioned hand-held sources. Additionally, fixed-site hover tests are carried out to determine if there are any differences in background. This procedure allows corrections to be applied to each survey flight, to eliminate any differences which might result from changes in temperature or humidity.

Radar Altimeter

Manufacturer:	Sperry
Model:	RT220
Type:	Short pulse modulation, 4.3 GHz
Sensitivity:	0.3 m

The radar altimeter measures the vertical distance between the helicopter and the ground. This information is used in the processing algorithm which determines conductor depth.

Barometric Pressure and Temperature Sensors

Model:	DIGHEM D 1300	
Type:	Motorola MPX4115AP analog pressure sensor AD592AN high-impedance remote temperature sensors	
Sensitivity:	Pressure: Temperature:	150 mV/kPa 100 mV/°C or 10 mV/°C (selectable)
Sample rate:	10 per second	

The D1300 circuit is used in conjunction with one barometric sensor and up to three temperature sensors. Two sensors (baro and temp) are installed in the EM console in the aircraft, to monitor pressure and internal operating temperatures.

Analog Recorder

Manufacturer:	RMS Instruments
Type:	DGR33 dot-matrix graphics recorder
Resolution:	4x4 dots/mm
Speed:	1.5 mm/sec

The analog profiles are recorded on chart paper in the aircraft during the survey. Table 2-1 lists the geophysical data channels and the vertical scale of each profile.

Table 2-1. The Analog Profiles

Channel Name	Parameter	Scale units/mm	Designation on Digital Profile
1X9I	coaxial in-phase (1000 Hz)	2.5 ppm	CXI1000
1X9Q	coaxial quad (1000 Hz)	2.5 ppm	CXQ1000
3P9I	coplanar in-phase (900 Hz)	2.5 ppm	CPI900
3P9Q	coplanar quad (900 Hz)	2.5 ppm	CPQ900
2P7I	coplanar in-phase (7200 Hz)	5 ppm	CPI7200
2P7Q	coplanar quad (7200 Hz)	5 ppm	CPQ7200
4X7I	coaxial in-phase (5500 Hz)	5 ppm	CXI5500
4X7Q	coaxial quad (5500 Hz)	5 ppm	CXQ5500
5P5I	coplanar in-phase (56000 Hz)	10 ppm	CPI56K
5P5Q	coplanar quad (56000 Hz)	10 ppm	CPQ56K
ALTR	altimeter (radar)	3 m	ALTBIRDM
MAGC	magnetics, coarse	20 nT	MAGFNL
MAGF	magnetics, fine	2.0 nT	MAG
CXSP	coaxial sferics monitor		CXSP
CPSP	coplanar sferics monitor		
CXPL	coaxial powerline monitor		
CPPL	coplanar powerline monitor		CPPL
TC	total counts	100 cps	
K	potassium	10 cps	
U	uranium	10 cps	
TH	thorium	10 cps	
1KPA	altimeter (barometric)	30 m	
2TDC	internal (console) temperature	1° C	
3TDC	external temperature	1° C	

Digital Data Acquisition System

Manufacturer: RMS Instruments

Model: DGR 33

Recorder: SCM Microsystems flash card drive

The data are stored on a 48 Mb flash card and are downloaded to the field workstation PC at the survey base for verification, backup and preparation of in-field products.

Video Flight Path Recording System

Type: Panasonic VHS Colour Video Camera (NTSC)

Model: AG 720/WVCL322

Fiducial numbers are recorded continuously and are displayed on the margin of each image. This procedure ensures accurate correlation of analog and digital data with respect to visible features on the ground.

Navigation (Global Positioning System)

Airborne Receiver

Model:	Ashtech Glonass GG24
Type:	SPS (L1 band), 24-channel, C/A code at 1575.42 MHz, S code at 0.5625 MHz, Real-time differential.
Sensitivity:	-132 dBm, 0.5 second update
Accuracy:	Manufacturer's stated accuracy is better than 10 metres real-time

Base Station

Model:	Ashtech Z-Surveyor
Type:	Dual frequency, 12 channels, full wavelength carrier on L1 and L2
Accuracy:	Manufacturer's stated accuracy for differential corrected GPS is <1 metre.

The Ashtech GG24 is a line of sight, satellite navigation system which utilizes time-coded signals from at least four of forty-eight available satellites. Both Russian GLONASS and American NAVSTAR satellite constellations are used to calculate the position and to provide real time guidance to the helicopter. The Ashtech system can be combined with a RACAL or similar GPS receiver which further improves the accuracy of the flying and subsequent flight path recovery to better than 5 metres. The differential corrections, which are obtained from a network of virtual reference stations, are transmitted to the helicopter

via a spot-beam satellite. This eliminates the need for a local GPS base station. However, the Ashtech Z-Surveyor was used as a backup to provide post-survey differential corrections.

The Ashtech Z-Surveyor is operated as a base station and utilizes time-coded signals from at least four of the twenty-four NAVSTAR satellites. The base station raw XYZ data are recorded, thereby permitting post-survey processing for theoretical accuracies of better than 1 metre.

The Ashtech receiver was coupled with a Picodas 2100 navigation system for real-time guidance.

Although the base station receiver is able to calculate its own latitude and longitude, a higher degree of accuracy can be obtained if the reference unit is established on a known benchmark or triangulation point. For this survey, the GPS station was located at latitude 56°58'25.67887"N, longitude 126°44'14.401"W at an elevation of 1286.75 metres a.m.s.l. The GPS records data relative to the WGS84 ellipsoid, which is the basis of the revised North American Datum (NAD83). Conversion software is used to transform the WGS84 coordinates to the NAD27 system displayed on the base maps.

Field Workstation

A PC is used at the survey base to verify data quality and completeness. Flight data are transferred to the PC hard drive to permit the creation of a database using a proprietary software package (typhoon-version 17.01.04). This process allows the field operators to display both the positional (flight path) and geophysical data on a screen or printer.

3. PRODUCTS AND PROCESSING TECHNIQUES

Table 3-1 lists the maps and products which have been provided under the terms of the survey agreement. Other products can be prepared from the existing dataset, if requested. These include magnetic enhancements or derivatives, percent magnetite, digital terrain or resistivity-depth sections. Most parameters can be displayed as contours, profiles, or in colour.

Base Maps

Base maps of the survey area have been produced from published topographic maps. These provide a relatively accurate, distortion-free base which facilitates correlation of the navigation data to the UTM grid. The original topographic maps are scanned to a bitmap format and combined with geophysical data for plotting the final maps. All maps are created using the following parameters:

Projection Description:

Datum:	NAD27 (ALTA & BC)
Ellipsoid:	Clarke 1866
Projection:	UTM (Zone: 9)
Central Meridian:	129°w
False Northing:	0
False Easting:	500000
Scale Factor:	0.9996
WGS84 to Local Conversion:	Molodensky
Datum Shifts:	DX: 7 DY: -162 DZ: -188

Table 3-1 Survey Products

1. Final Transparent Maps (+3 prints) @ 1:20,000

   Dighem EM anomalies
   Total magnetic field
   Calculated vertical magnetic gradient
   Apparent resistivity (900 Hz)
   Apparent resistivity (7200 Hz)

2. Colour Maps (2 sets) @ 1:20,000

   Total magnetic field
   Calculated vertical magnetic gradient
   Apparent resistivity (900 Hz)
   Apparent resistivity (7200 Hz)
   Radiometric Potassium Counts
   Radiometric Uranium Counts
   Radiometric Thorium Counts
   Radiometric Total Count

3. Additional Products

   Digital XYZ archive in Geosoft format (CD-ROM)
   Digital grid archives in Geosoft format (CD-ROM)
   Survey logistics report (3 copies)
   Multi-channel stacked profiles
   Analog chart records
   Flight path video cassettes

Note: Other products can be produced from existing survey data, if requested.

Electromagnetic Anomalies

EM data are processed at the recorded sample rate of 10 samples/second. If necessary, appropriate spheric rejection median or Hanning filters are applied to reduce noise to acceptable levels. EM test profiles are then created to allow the interpreter to select the most appropriate EM anomaly picking controls for a given survey area. The EM picking parameters depend on several factors but are primarily based on the dynamic range of the resistivities within the survey area, and the types and expected geophysical responses of the targets being sought.

Anomalous electromagnetic responses are selected and analysed by computer to provide a preliminary electromagnetic anomaly map. The automatic selection algorithm is intentionally oversensitive to assure that no meaningful responses are missed. Using the preliminary map in conjunction with the multi-parameter stacked profiles, the interpreter then classifies the anomalies according to their source and eliminates those that are not substantiated by the data. The final interpreted EM anomaly map includes bedrock, surficial and cultural conductors. A map containing only bedrock conductors can be generated, if desired.

Apparent Resistivity

The apparent resistivity in ohm-m can be generated from the in-phase and quadrature EM components for any of the frequencies, using a pseudo-layer half-space model. A resistivity map portrays all the EM information for that frequency over the entire survey area. This contrasts with the electromagnetic anomaly map which provides information only over interpreted conductors. The large dynamic range makes the resistivity parameter an excellent mapping tool.

The preliminary resistivity maps and images are carefully inspected to locate any lines or line segments which might require levelling adjustments. Subtle changes between in-flight calibrations of the system can result in line to line differences, particularly in resistive (low signal amplitude) areas. If required, manual levelling is carried out to eliminate or minimize resistivity differences which can be caused by changes in operating temperatures. These levelling adjustments are usually very subtle, and do not result in the degradation of anomalies from valid bedrock sources.

After the manual levelling process is complete, revised resistivity grids are created. The resulting grids can be subjected to a microlevelling filter in order to smooth the data for contouring. The coplanar resistivity parameter has a broad 'footprint' which requires very little filtering.

The calculated resistivities for the three coplanar frequencies are included in the XYZ and grid archives. Values are in ohm-metres on all final products.

Total Magnetic Field

The aeromagnetic data are corrected for diurnal variation using the magnetic base station data. Manual adjustments are applied to any lines that require levelling, as indicated by shadowed images of the gridded magnetic data or tie line/traverse line intercepts. The IGRF gradient can be removed from the corrected total field data, if requested.

Calculated Vertical Magnetic Gradient

The diurnally-corrected total magnetic field data are subjected to a processing algorithm which enhances the response of magnetic bodies in the upper 500 m and attenuates the response of deeper bodies. The resulting vertical gradient map provides better definition and resolution of near-surface magnetic units. It also identifies weak magnetic features which may not be evident on the total field map. However, regional magnetic variations and changes in lithology may be better defined on the total magnetic field map.

Magnetic Derivatives (optional)

The total magnetic field data can be subjected to a variety of filtering techniques to yield maps of the following:

enhanced magnetics

second vertical derivative

reduction to the pole/equator

magnetic susceptibility with reduction to the pole

upward/downward continuations

analytic signal

All of these filtering techniques improve the recognition of near-surface magnetic bodies, with the exception of upward continuation. Any of these parameters can be produced on request. Dighem's proprietary enhanced magnetic technique is designed to provide a general "all-purpose" map, combining the more useful features of the above parameters.

Radiometrics

All radiometric data reductions performed by Dighem rigorously follow the procedures described in the IAEA Technical Report[1].

All processing of radiometric data was undertaken at the natural sampling rate of the spectrometer, i.e., one second. The data were not interpolated to match the fundamental 0.1 second interval of the EM and magnetic data.

The following sections describe each step in the process.

Pre-filtering

The radar altimeter data were processed with a 49-point median filter to remove spikes.

Reduction to Standard Temperature and Pressure

The radar altimeter data were converted to effective height (h_e) in feet using the acquired temperature and pressure data, according to the following formula:

$$h_e = h * \frac{273.15}{T + 273.15} * \frac{P}{1013.25}$$

---

[1] Exploranium, I.A.E.A. Report, Airborne Gamma-Ray Spectrometer Surveying, Technical Report No. 323, 1991.

where: h is the observed crystal to ground distance in feet

T is the measured air temperature in degrees Celsius

P is the barometric pressure in millibars

Live Time Correction

The spectrometer, an Exploranium GR-820, uses the notion of "live time" to express the relative period of time the instrument was able to register new pulses per sample interval. This is the opposite of the traditional "dead time", which is an expression of the relative period of time the system was unable to register new pulses per sample interval.

The GR-820 measures the live time electronically, and outputs the value in milliseconds. The live time correction is applied to the total count, potassium, uranium, thorium, upward uranium and cosmic channels. The formula used to apply the correction is as follows:

$$C_{lt} = C_{raw} * \frac{1000.0}{L}$$

where: C_{lt} is the live time corrected channel in counts per second

C_{raw} is the raw channel data in counts per second

L is the live time in milliseconds

Intermediate Filtering

Two parameters were filtered, but not returned to the database:

- Radar altimeter was smoothed with a 5-point Hanning filter (h_{ef}).
- The Cosmic window was smoothed with a 29-point Hanning filter (Cos_f).

Aircraft and Cosmic Background

Aircraft background and cosmic stripping corrections were applied to the total count, potassium, uranium, thorium and upward uranium channels using the following formula:

$$C_{ac} = C_{lt} - (a_c + b_c * \mathrm{Cos}_f)$$

where: C_{ac} is the background and cosmic corrected channel

C_{lt} is the live time corrected channel

a_c is the aircraft background for this channel

b_c is the cosmic stripping coefficient for this channel

Cos_f is the filtered Cosmic channel

Radon Background

The determination of calibration constants that enable the stripping of the effects of atmospheric radon from the downward-looking detectors through the use of an upward-looking detector is divided into two parts:

1) Determine the relationship between the upward- and downward-looking detector count rates for radiation originating from the ground.

2) Determine the relationship between the upward- and downward-looking detector count rates for radiation due to atmospheric radon.

The procedures to determine these calibration factors are documented in IAEA Report #323 on airborne gamma-ray surveying. The calibrations for the first part were determined as outlined in the report.

The latter case normally requires many over-water measurements where there is no contribution from the ground. Where this is not possible, it is standard procedure to establish a test line over which a series of repeat measurements are acquired. From these repeat flights, any change in the downward uranium window due to variations in radon background would be directly related to variations in the upward window and the other downward windows.

The validity of this technique rests on the assumption that the radiation from the ground is essentially constant from flight to flight. Inhomogeneities in the ground, coupled with deviations in the flight path between test runs, add to the inaccuracy of the accumulated results. Variations in flying heights and other environmental factors also contribute to the uncertainty.

The use of test lines is a solution for a fixed-wing acquisition platform. The ability of rotary wing platforms to hover at a constant height over a fixed position would appear to eliminate a number of the variations which degrade the accuracy of the results required for this calibration.

Hover test sites were established in or near the survey area. The tests were carried out at the start and end of each day, and at the end of each flight. Data were acquired over a four minute period at the nominal survey altitude (60 m). The data were then corrected for livetime, aircraft background and cosmic activity.

Once the survey was completed, the relationships between the counts in the downward uranium window and in the other four windows due to atmospheric radon were determined using linear regression for each of the three hover sites. The equations solved for were:

$$u_r = a_u Ur + b_u$$

$$K_r = a_K U_r + b_K$$

$$T_r = a_T U_r + b_T$$

$$I_r = a_I U_r + b_I$$

where: u_r is the radon component in the upward uranium window

K_r, U_r, T_r and I_r are the radon components in the various windows of the downward detectors

the various "a" and "b" coefficients are the required calibration constants

In practice, only the "a" constants were used in the final processing. The "b" constants, which are normally near zero for over-water calibrations, were of no value as they reflected the local distribution of the ground concentrations measured in the five windows.

The thorium, uranium and upward uranium data for each line were copied into temporary arrays, then smoothed with 21, 21 and 51 point Hanning filters to product Th_f, U_f, and u_f respectively. The radon component in the downward uranium window was then determined using the following formula:

$$U_r = \frac{u_f - a_1 * U_f - a_2 * Th_f + a_2 * b_{Th} - b_u}{a_u - a_1 - a_2 * a_{Th}}$$

where: U_r is the radon component in the downward uranium window

u_f is the filtered upward uranium

U_f is the filtered uranium

Th_f is the filtered thorium

a_1, a_2, a_u and a_{Th} are proportionality factors and

b_u and b_{Th} are constants determined experimentally

The effects of radon in the downward uranium are removed by simply subtracting U_r from U_{ac}. The effects of radon in the total count, potassium, thorium and upward uranium are then removed based upon previously established relationships with U_r. The corrections are applied using the following formula:

$$C_{rc} = C_{ac} - (a_c * U_r + b_c)$$

where: C_{rc} is the radon corrected channel

C_{ac} is the background and cosmic corrected channel

U_r is the radon component in the downward uranium window

a_c is the proportionality factor and

b_c is the constant determined experimentally for this channel

Compton Stripping

Following the radon correction, the potassium, uranium and thorium are corrected for spectral overlap. First, α,β and γ the stripping ratios, are modified according to altitude. Then an adjustment factor based on a, the reversed stripping ratio, uranium into thorium, is calculated. (Note: the stripping ratio altitude correction constants are expressed in change per metre. A constant of 0.3048 is required to conform to the internal usage of height in feet):

$$\alpha_h = \alpha + h_{ef} * 0.00049$$

$$\alpha_r = \frac{1.0}{1.0 - a * \alpha_h}$$

$$\beta_h = \beta + h_{ef} * 0.00065$$

$$\gamma_h = \gamma + h_{ef} * 0.00069$$

where: α, β, γ are the Compton stripping coefficients

α_h, β_h, γ_h are the height corrected Compton stripping coefficients

h_{ef} is the height above ground in metres

α_r is the scaling factor correcting for back scatter

a is the reverse stripping ratio

The stripping corrections are then carried out using the following formulas:

$$Th_c = (Th_{rc} - a * U_{rc}) * \alpha_r$$

$$K_c = K_{rc} - \gamma_h * U_c - \beta_h * Th_c$$

$$U_c = (U_{rc} - \alpha_h * Th_{rc}) * \alpha_r$$

where: U_c, Th_c and K_c are corrected uranium, thorium and potassium

$\alpha_h, \beta_h, \gamma_h$ are the height corrected Compton stripping coefficients

U_{rc}, Th_{rc} and K_{rc} are radon-corrected uranium, thorium and potassium

α_r is the backscatter correction

Attenuation Corrections

The total count, potassium, uranium and thorium data are then corrected to a nominal survey altitude, in this case 200 feet. This is done according to the equation:

$$C_a = C * e^{\mu(h_{ef} - ho)}$$

where: C_a is the output altitude corrected channel

C is the input channel

$e\mu$ is the attenuation correction for that channel

h_{ef} is the effective altitude

h_0 is the nominal survey altitude to correct to

Adjustments

Manual adjustments may have been to the data in some parts of the survey area to minimize the effect of the problems which were not completely eliminated by the standard processing. However, the data may be of lower reliability in the areas covered by the affected lines.

All coefficients used in processing the radiometric data are included in the Radiometric Processing Control Files appended to this report.

Multi-channel Stacked Profiles

Distance-based profiles of the digitally recorded geophysical data are generated and plotted by computer. These profiles also contain the calculated parameters which are used in the interpretation process. These are produced as worksheets prior to interpretation, and are also presented in the final corrected form after interpretation. The profiles display electromagnetic anomalies with their respective interpretive symbols. Table 3-2 shows the parameters and scales for the multi-channel stacked profiles.

In Table 3-2, the log resistivity scale of 0.06 decade/mm means that the resistivity changes by an order of magnitude in 16.6 mm. The resistivities at 0, 33 and 67 mm up from the bottom of the digital profile are respectively 1, 100 and 10,000 ohm-m.

Table 3-2. Multi-channel Stacked Profiles

Channel Name (Freq)	Observed Parameters	Scale Units/mm
MAGFNL	total magnetic field	20 nT
ALTBIRDM	EM sensor height above ground	6 m
CXI1000	vertical coaxial coil-pair in-phase (1000 Hz)	5 ppm
CXQ1000	vertical coaxial coil-pair quadrature (900 Hz)	5 ppm
CPI900	horizontal coplanar coil-pair in-phase (900 Hz)	10 ppm
CPQ900	horizontal coplanar coil-pair quadrature (900 Hz)	10 ppm
CXI5500	vertical coaxial coil-pair in-phase (5500 Hz)	10 ppm
CXQ5500	vertical coaxial coil-pair quadrature (5500 Hz)	10 ppm
CPI7200	horizontal coplanar coil-pair in-phase (7200 Hz)	20 ppm
CPQ7200	horizontal coplanar coil-pair quadrature (7200 Hz)	20 ppm
CPI56K	horizontal coplanar coil-pair in-phase (56,000 Hz)	30 ppm
CPQ56K	horizontal coplanar coil-pair quadrature (56,000 Hz)	30 ppm
CXSP	coaxial spherics monitor	
CPPL	coplanar powerline monitor	
	Computed Parameters	
DIFI (5500/7200 Hz)	difference function in-phase from CXI and CPI	10 ppm
DIFQ (5500/7200 Hz)	difference function quadrature from CXQ and CPQ	10 ppm
RES900	log resistivity	.06 decade
RES7200	log resistivity	.06 decade
RES56K	log resistivity	.06 decade
DEP900	apparent depth	6 m
DEP7200	apparent depth	6 m
DEP56K	apparent depth	6 m
CDT	conductance	1 grade

Contour, Colour and Shadow Map Displays

The geophysical data are interpolated onto a regular grid using a modified Akima spline technique. The resulting grid is suitable for generating contour maps of excellent quality. The grid cell size is usually 25% of the line interval.

Colour maps are produced by interpolating the grid down to the pixel size. The parameter is then incremented with respect to specific amplitude ranges to provide colour "contour" maps. Colour maps of the total magnetic field are particularly useful in defining the lithology of the survey area.

Monochromatic shadow maps or images are generated by employing an artificial sun to cast shadows on a surface defined by the geophysical grid. There are many variations in the shadowing technique. These techniques can be applied to total field or enhanced magnetic data, magnetic derivatives, VLF, resistivity, etc. The shadow of the enhanced magnetic parameter is particularly suited for defining geological structures with crisper images and improved resolution.

Resistivity-depth Sections

The apparent resistivities for all frequencies can be displayed simultaneously as coloured resistivity-depth sections. Usually, only the coplanar data are displayed as the close

frequency separation between the coplanar and adjacent coaxial data tends to distort the section. The sections can be plotted using the topographic elevation profile as the surface. The digital terrain values, in metres a.m.s.l., can be calculated from the GPS z-value or barometric altimeter, minus the aircraft radar altimeter.

Resistivity-depth sections can be generated in three formats:

(1) Sengpiel resistivity sections, where the apparent resistivity for each frequency is plotted at the depth of the centroid of the in-phase current flow[2]; and,

(2) Differential resistivity sections, where the differential resistivity is plotted at the differential depth[3].

(3) Occam[4] or Multi-layer[5] inversion.

Both the Sengpiel and differential methods are derived from the pseudo-layer half-space model. Both yield a coloured resistivity-depth section which attempts to portray a smoothed approximation of the true resistivity distribution with depth. Resistivity-depth

---

2 Sengpiel, K.P., 1988, Approximate Inversion of Airborne EM Data from Multilayered Ground: Geophysical Prospecting 36, 446-459.

3 Huang, H. and Fraser, D.C., 1993, Differential Resistivity Method for Multi-frequency Airborne EM Sounding: presented at Intern. Airb. EM Workshop, Tucson, Ariz.

4 Constable et al, 1987, Occam's inversion: a practical algorithm for generating smooth models from electromagnetic sounding data: Geophysics, 52, 289-300.

5 Huang H., and Palacky, G.J., 1991, Damped least-squares inversion of time domain airborne EM data based on singular value decomposition: Geophysical Prospecting, 39, 827-844.

sections are most useful in conductive layered situations, but may be unreliable in areas of moderate to high resistivity where signal amplitudes are weak. In areas where in-phase responses have been suppressed by the effects of magnetite, the computed resistivities shown on the sections may be unreliable. The differential resistivity technique was developed by Dighem. It is more sensitive than the Sengpiel section to changes in the earth's resistivity and it reaches deeper.

Both the Occam and Multi-layer Inversions compute the layered earth resistivity model which would best match the measured EM data. The Occam inversion uses a series of thin, fixed layers (usually 20 x 5m and 10 x 10m layers) and computes resistivities to fit the EM data. The multi-layer inversion computes the resistivity and thickness for each of a defined number of layers (typically 3-5 layers) to best fit the data.

4. SURVEY RESULTS

General Discussion

The survey results are presented on separate map sheets for each parameter at a scale of 1:20,000. Table 4-1 summarizes the EM responses in the survey areas, with respect to conductance grade and interpretation.

The anomalies shown on the electromagnetic anomaly maps are based on a near-vertical, half plane model. This model best reflects "discrete" bedrock conductors. Wide bedrock conductors or flat-lying conductive units, whether from surficial or bedrock sources, may give rise to very broad anomalous responses on the EM profiles. These may not appear on the electromagnetic anomaly map if they have a regional character rather than a locally anomalous character. These broad conductors, which more closely approximate a half-space model, will be maximum coupled to the horizontal (coplanar) coil-pair and should be more evident on the resistivity parameter. Resistivity maps, therefore, may be more valuable than the electromagnetic anomaly maps, in areas where broad or flat-lying conductors are considered to be of importance. Contoured resistivity maps, based on the 900 Hz and 7200 Hz coplanar data are included with this report.

TABLE 4-1 EM ANOMALY STATISTICS

BRENDA PROPERTY, JOCK CREEK, B.C.

CONDUCTOR GRADE	CONDUCTANCE RANGE SIEMENS (MHOS)	NUMBER OF RESPONSES
7	>100	0
6	50 - 100	0
5	20 - 50	0
4	10 - 20	0
3	5 - 10	0
2	1 - 5	16
1	<1	101
*	INDETERMINATE	191
TOTAL		308

CONDUCTOR MODEL	MOST LIKELY SOURCE	NUMBER OF RESPONSES
D	DISCRETE BEDROCK CONDUCTOR	2
B	DISCRETE BEDROCK CONDUCTOR	17
S	CONDUCTIVE COVER	289
TOTAL		308

(SEE EM MAP LEGEND FOR EXPLANATIONS)

TABLE 4-2 EM ANOMALY STATISTICS

KEMESS MINE PROPERTY, B.C.

CONDUCTOR GRADE	CONDUCTANCE RANGE SIEMENS (MHOS)	NUMBER OF RESPONSES
7	>100	0
6	50 - 100	0
5	20 - 50	4
4	10 - 20	7
3	5 - 10	39
2	1 - 5	368
1	<1	382
*	INDETERMINATE	511
TOTAL		1311

CONDUCTOR MODEL	MOST LIKELY SOURCE	NUMBER OF RESPONSES
D	DISCRETE BEDROCK CONDUCTOR	28
B	DISCRETE BEDROCK CONDUCTOR	233
S	CONDUCTIVE COVER	940
E	EDGE OF WIDE CONDUCTOR	1
L	CULTURE	109
TOTAL		1311

(SEE EM MAP LEGEND FOR EXPLANATIONS)

TABLE 4-3 EM ANOMALY STATISTICS

KG PROPERTY, McCONNELL CREEK, B.C.

CONDUCTOR GRADE	CONDUCTANCE RANGE SIEMENS (MHOS)	NUMBER OF RESPONSES
7	>100	0
6	50 - 100	0
5	20 - 50	0
4	10 - 20	2
3	5 - 10	1
2	1 - 5	52
1	<1	67
*	INDETERMINATE	153
TOTAL		275

CONDUCTOR MODEL	MOST LIKELY SOURCE	NUMBER OF RESPONSES
D	DISCRETE BEDROCK CONDUCTOR	16
B	DISCRETE BEDROCK CONDUCTOR	68
S	CONDUCTIVE COVER	191
TOTAL		275

(SEE EM MAP LEGEND FOR EXPLANATIONS)

TABLE 4-4 EM ANOMALY STATISTICS

CROY PROPERTY, KLIYUL CREEK, B.C.

CONDUCTOR GRADE	CONDUCTANCE RANGE SIEMENS (MHOS)	NUMBER OF RESPONSES
7	>100	0
6	50 - 100	0
5	20 - 50	0
4	10 - 20	3
3	5 - 10	4
2	1 - 5	32
1	<1	42
*	INDETERMINATE	329
TOTAL		410

CONDUCTOR MODEL	MOST LIKELY SOURCE	NUMBER OF RESPONSES
D	DISCRETE BEDROCK CONDUCTOR	1
B	DISCRETE BEDROCK CONDUCTOR	11
S	CONDUCTIVE COVER	398
TOTAL		410

(SEE EM MAP LEGEND FOR EXPLANATIONS)

Excellent resolution and discrimination of conductors was accomplished by using a fast sampling rate of 0.1 sec and by employing a common frequency (5500 Hz and 7200 Hz) on two orthogonal coil-pairs (coaxial and coplanar). The resulting "difference channel" parameters often permit differentiation of bedrock and surficial conductors, even though they may exhibit similar conductance values.

Anomalies which occur near the ends of the survey lines (i.e., outside the survey area), should be viewed with caution. Some of the weaker anomalies could be due to aerodynamic noise, i.e., bird bending, which is created by abnormal stresses to which the bird is subjected during the climb and turn of the aircraft between lines. Such aerodynamic noise is usually manifested by an anomaly on the coaxial in-phase channel only, although severe stresses can affect the coplanar in-phase channels as well.

Magnetics

A Fugro CF1 cesium vapour magnetometer was operated at the survey base to record diurnal variations of the earth's magnetic field. The clock of the base station was synchronized with that of the airborne system to permit subsequent removal of diurnal drift. A GEM Systems GSM-19T proton precession magnetometer was also operated as a backup unit.

The total magnetic field data have been presented as contours on the base maps using a contour interval of 5 nT where gradients permit. The maps show the magnetic properties of the rock units underlying the survey areas.

The total magnetic field data have been subjected to a processing algorithm to produce maps of the calculated vertical gradient. This procedure enhances near-surface magnetic units and suppresses regional gradients. It also provides better definition and resolution of magnetic units and displays weak magnetic features which may not be clearly evident on the total field maps.

There is some evidence on the magnetic maps which suggests that the survey areas have been subjected to deformation and/or alteration. These structural complexities are evident on the contour maps as variations in magnetic intensity, irregular patterns, and as offsets or changes in strike direction.

If a specific magnetic intensity can be assigned to the rock type which is believed to host the target mineralization, it may be possible to select areas of higher priority on the basis of the total field magnetic data. This is based on the assumption that the magnetite content of the host rocks will give rise to a limited range of contour values which will permit differentiation of various lithological units.

The magnetic results, in conjunction with the other geophysical parameters, have provided valuable information which can be used to effectively map the geology and structure in the survey areas.

Apparent Resistivity

Apparent resistivity maps, which display the conductive properties of the survey area, were produced from the 900 Hz and 7200 Hz coplanar data. The maximum resistivity values, which are calculated for each frequency, are 1,035 and 8,180 ohm-m respectively. These cutoffs eliminate the erratic higher resistivities which would result from unstable ratios of very small EM amplitudes.

There are other resistivity lows in the area. Some of these are quite extensive and often reflect "formational" conductors which may be of minor interest as direct exploration targets. However, attention may be focused on areas where these zones appear to be faulted or folded or where anomaly characteristics differ along strike.

Electromagnetic Anomalies

Problems with the visual quality of the video tapes were encountered. Portions of the video tapes were able to be viewed with some difficulty, allowing positive identification of

anomalies in some areas. Those that could not be positively identified are classified with a "?" symbol.

The EM anomalies resulting from this survey appear to fall within one of three general categories. The first type consists of discrete, well-defined anomalies which yield marked inflections on the difference channels. These anomalies are usually attributed to conductive sulphides or graphite and are generally given a "B", "T" or "D" interpretive symbol, denoting a bedrock source.

The second class of anomalies comprises moderately broad responses which exhibit the characteristics of a half-space and do not yield well-defined inflections on the difference channels. Anomalies in this category are usually given an "S" or "H" interpretive symbol. The lack of a difference channel response usually implies a broad or flat-lying conductive source such as overburden. Some of these anomalies may reflect conductive rock units, zones of deep weathering, or the weathered tops of kimberlite pipes which can often yield "non-discrete" signatures.

The effects of conductive overburden are evident over portions of the survey area. Although the difference channels (DIFI and DIFQ) are extremely valuable in detecting bedrock conductors which are partially masked by conductive overburden, sharp undulations in the bedrock/overburden interface can yield anomalies in the difference channels which may be interpreted as possible bedrock conductors. Such anomalies

usually fall into the "S?" or "B?" classification but may also be given an "E" interpretive symbol, denoting a resistivity contrast at the edge of a conductive unit.

The "?" symbol does not question the validity of an anomaly, but instead indicates some degree of uncertainty as to which is the most appropriate EM source model. This ambiguity results from the combination of effects from two or more conductive sources, such as overburden and bedrock, gradational changes, or moderately shallow dips. The presence of a conductive upper layer has a tendency to mask or alter the characteristics of bedrock conductors, making interpretation difficult. This problem is further exacerbated in the presence of magnetite.

In areas where EM responses are evident primarily on the quadrature components, zones of poor conductivity are indicated. Where these responses are coincident with magnetic anomalies, it is possible that the in-phase component amplitudes have been suppressed by the effects of magnetite. Most of these poorly-conductive magnetic features give rise to resistivity anomalies which are only slightly below background. If it is expected that poorly-conductive economic mineralization may be associated with magnetite-rich units, most of these weakly anomalous features will be of interest. In areas where magnetite causes the in-phase components to become negative, the apparent conductance and depth of EM anomalies may be unreliable. Magnetite effects usually give rise to overstated (higher) resistivity values and understated (shallow) depth calculations.

The third class consists of cultural anomalies which are usually given the symbol "L" or "L?".

It is recommended that an attempt be made to compile a suite of geophysical "signatures" over any known areas of interest. Anomaly characteristics are clearly defined on the computer-processed geophysical data profiles which are supplied as one of the survey products.

A complete assessment and evaluation of the survey data should be carried out by one or more qualified professionals who have access to, and can provide a meaningful compilation of, all available geophysical, geological and geochemical data.

Conductors in the Survey Area

The electromagnetic anomaly maps show the anomaly locations with the interpreted conductor type, dip, conductance and depth being indicated by symbols. Direct magnetic correlation is also shown if it exists. The strike direction and length of the conductors are indicated where anomalies can be correlated from line to line with a reasonable degree of confidence.

5. CONCLUSIONS AND RECOMMENDATIONS

This report provides a very brief description of the equipment, procedures and logistics of the survey.

There are a few conductive anomalies in the survey blocks that may be of interest. The survey was also successful in locating a few moderately weak or broad conductors which may warrant additional work. The various maps included with this report display the magnetic, conductive and radiometric properties of the survey areas. It is recommended that the survey results be reviewed in detail, in conjunction with all available geophysical, geological and geochemical information. Particular reference should be made to the computer generated data profiles which clearly define the characteristics of the individual anomalies.

Most anomalies in the area are moderately weak and poorly-defined. Many have been attributed to conductive overburden or deep weathering, although a few appear to be associated with magnetite-rich rock units. Others coincide with magnetic gradients which may reflect contacts, faults or shears. Such structural breaks are considered to be of particular interest as they may have influenced mineral deposition within the survey area.

The interpreted bedrock conductors defined by the survey should be subjected to further investigation, using appropriate surface exploration techniques. Anomalies which are

currently considered to be of moderately low priority may require upgrading if follow-up results are favourable.

It is also recommended that image processing of existing geophysical data be considered, in order to extract the maximum amount of information from the survey results. Current software and imaging techniques often provide valuable information on structure and lithology, which may not be clearly evident on the contour and colour maps. These techniques can yield images which define subtle, but significant, structural details.

Respectfully submitted,

FUGRO AIRBORNE SURVEYS CORP.

Mark Stephens, M.Sc.
Geophysicist

MS/sdp

R2116OCT.02

APPENDIX A

LIST OF PERSONNEL

The following personnel were involved in the acquisition, processing, interpretation and presentation of data, relating to a DIGHEM$^{V\text{-}DSP}$ airborne geophysical survey carried out for Northgate Exploration Limited in the Toodoggone Area, British Columbia.

David Miles	Manager, Helicopter Operations
Emily Farquhar	Manager, Data Processing and Interpretation
Michael Senko	Senior Geophysical Operator
Nick Venter	Field Geophysicist
Terry Thompson	Pilot (Questral Helicopters Ltd.)
Doug Naismith	Engineer (Questral Helicopters Ltd.)
Gordon Smith	Data Processing Supervisor
Gordon Smith	Computer Processor
Mark Stephens	Interpretation Geophysicist
Lyn Vanderstarren	Drafting Supervisor
Susan Pothiah	Word Processing Operator
Albina Tonello	Secretary/Expeditor

The survey consisted of 1824.4 km of coverage, flown from August 12 to August 18, 2002.

All personnel are employees of Fugro Airborne Surveys, except for the pilot and engineer who are employees of Questral Helicopters Ltd.

APPENDIX B

STATEMENT OF COST

Date: October 29, 2002

IN ACCOUNT WITH FUGRO AIRBORNE SURVEYS

To: Fugro flying of Agreement dated July 17, 2002, pertaining to an Airborne Geophysical Survey in the Toodoggone area, British Columbia.

Survey Charges

Mobilization/demobilization	$ 10,000.00
1746 km of flying @ $99.00/km	$ 172,854.00
	$ 182,854.00

Allocation of Costs

- Data Acquisition	(80%)
- Data Processing	(10%)
- Interpretation, Report and Maps	(10%)

- Appendix C.1 -

BACKGROUND INFORMATION

Electromagnetics

DIGHEM electromagnetic responses fall into two general classes, discrete and broad. The discrete class consists of sharp, well-defined anomalies from discrete conductors such as sulphide lenses and steeply dipping sheets of graphite and sulphides. The broad class consists of wide anomalies from conductors having a large horizontal surface such as flatly dipping graphite or sulphide sheets, saline water-saturated sedimentary formations, conductive overburden and rock, and geothermal zones. A vertical conductive slab with a width of 200 m would straddle these two classes.

The vertical sheet (half plane) is the most common model used for the analysis of discrete conductors. All anomalies plotted on the geophysical maps are analyzed according to this model. The following section entitled **Discrete Conductor Analysis** describes this model in detail, including the effect of using it on anomalies caused by broad conductors such as conductive overburden.

The conductive earth (half-space) model is suitable for broad conductors. Resistivity contour maps result from the use of this model. A later section entitled **Resistivity Mapping** describes the method further, including the effect of using it on anomalies caused by discrete conductors such as sulphide bodies.

Geometric Interpretation

The geophysical interpreter attempts to determine the geometric shape and dip of the conductor. Figure C-1 shows typical DIGHEM anomaly shapes which are used to guide the geometric interpretation.

Discrete Conductor Analysis

The EM anomalies appearing on the electromagnetic map are analyzed by computer to give the conductance (i.e., conductivity-thickness product) in siemens (mhos) of a vertical sheet model. This is done regardless of the interpreted geometric shape of the conductor. This is not an unreasonable procedure, because the computed conductance increases as the electrical quality of the conductor increases, regardless of its true shape. DIGHEM anomalies are divided into seven grades of conductance, as shown in Table C-1. The conductance in siemens (mhos) is the reciprocal of resistance in ohms.

The conductance value is a geological parameter because it is a characteristic of the conductor alone. It generally is independent of frequency, flying height or depth of burial, apart from the averaging over a greater portion of the conductor as height increases. Small anomalies from deeply buried strong conductors are not confused with small anomalies from shallow weak conductors because the former will have larger conductance values.

Table C-1. EM Anomaly Grades

Anomaly Grade	Siemens
7	> 100
6	50 - 100
5	20 - 50
4	10 - 20
3	5 - 10
2	1 - 5
1	< 1

Conductive overburden generally produces broad EM responses which may not be shown as anomalies on the geophysical maps. However, patchy conductive overburden in otherwise resistive areas can yield discrete anomalies with a conductance grade (cf. Table C-1) of 1, 2 or even 3 for conducting clays which have resistivities as low as 50 ohm-m. In areas where ground resistivities are below 10 ohm-m, anomalies caused by weathering variations and similar causes can have any conductance grade. The anomaly shapes from the multiple coils often allow such conductors to be recognized, and these are indicated by the letters S, H, and sometimes E on the geophysical maps (see EM legend on maps).

For bedrock conductors, the higher anomaly grades indicate increasingly higher conductances. Examples: DIGHEM's New Insco copper discovery (Noranda, Canada) yielded a grade 5 anomaly, as did the neighbouring copper-zinc Magusi River ore body; Mattabi (copper-zinc, Sturgeon Lake, Canada) and Whistle (nickel, Sudbury, Canada) gave grade 6; and DIGHEM's Montcalm nickel-copper discovery (Timmins, Canada)

yielded a grade 7 anomaly. Graphite and sulphides can span all grades but, in any particular survey area, field work may show that the different grades indicate different types of conductors.

Strong conductors (i.e., grades 6 and 7) are characteristic of massive sulphides or graphite. Moderate conductors (grades 4 and 5) typically reflect graphite or sulphides of a less massive character, while weak bedrock conductors (grades 1 to 3) can signify poorly connected graphite or heavily disseminated sulphides. Grades 1 and 2 conductors may not respond to ground EM equipment using frequencies less than 2000 Hz.

The presence of sphalerite or gangue can result in ore deposits having weak to moderate conductances. As an example, the three million ton lead-zinc deposit of Restigouche Mining Corporation near Bathurst, Canada, yielded a well-defined grade 2 conductor. The 10 percent by volume of sphalerite occurs as a coating around the fine grained massive pyrite, thereby inhibiting electrical conduction. Faults, fractures and shear zones may produce anomalies which typically have low conductances (e.g., grades 1 to 3). Conductive rock formations can yield anomalies of any conductance grade. The conductive materials in such rock formations can be salt water, weathered products such as clays, original depositional clays, and carbonaceous material.

For each interpreted electromagnetic anomaly on the geophysical maps, a letter identifier and an interpretive symbol are plotted beside the EM grade symbol. The horizontal rows of dots, under the interpretive symbol, indicate the anomaly amplitude on the flight record.

The vertical column of dots, under the anomaly letter, gives the estimated depth. In areas where anomalies are crowded, the letter identifiers, interpretive symbols and dots may be obliterated. The EM grade symbols, however, will always be discernible, and the obliterated information can be obtained from the anomaly listing appended to this report.

The purpose of indicating the anomaly amplitude by dots is to provide an estimate of the reliability of the conductance calculation. Thus, a conductance value obtained from a large ppm anomaly (3 or 4 dots) will tend to be accurate whereas one obtained from a small ppm anomaly (no dots) could be quite inaccurate. The absence of amplitude dots indicates that the anomaly from the coaxial coil-pair is 5 ppm or less on both the in-phase and quadrature channels. Such small anomalies could reflect a weak conductor at the surface or a stronger conductor at depth. The conductance grade and depth estimate illustrates which of these possibilities fits the recorded data best.

The conductance measurement is considered more reliable than the depth estimate. There are a number of factors which can produce an error in the depth estimate, including the averaging of topographic variations by the altimeter, overlying conductive overburden, and the location and attitude of the conductor relative to the flight line. Conductor location and attitude can provide an erroneous depth estimate because the stronger part of the conductor may be deeper or to one side of the flight line, or because it has a shallow dip. A heavy tree cover can also produce errors in depth estimates. This is because the depth estimate is computed as the distance of bird from conductor, minus the altimeter reading.

The altimeter can lock onto the top of a dense forest canopy. This situation yields an erroneously large depth estimate but does not affect the conductance estimate.

Dip symbols are used to indicate the direction of dip of conductors. These symbols are used only when the anomaly shapes are unambiguous, which usually requires a fairly resistive environment.

A further interpretation is presented on the EM map by means of the line-to-line correlation of bedrock anomalies, which is based on a comparison of anomaly shapes on adjacent lines. This provides conductor axes which may define the geological structure over portions of the survey area. The absence of conductor axes in an area implies that anomalies could not be correlated from line to line with reasonable confidence.

DIGHEM electromagnetic anomalies are designed to provide a correct impression of conductor quality by means of the conductance grade symbols. The symbols can stand alone with geology when planning a follow-up program. The actual conductance values are printed in the attached anomaly list for those who wish quantitative data. The anomaly ppm and depth are indicated by inconspicuous dots which should not distract from the conductor patterns, while being helpful to those who wish this information. The map provides an interpretation of conductors in terms of length, strike and dip, geometric shape, conductance, depth, and thickness. The accuracy is comparable to an interpretation from a high quality ground EM survey having the same line spacing.

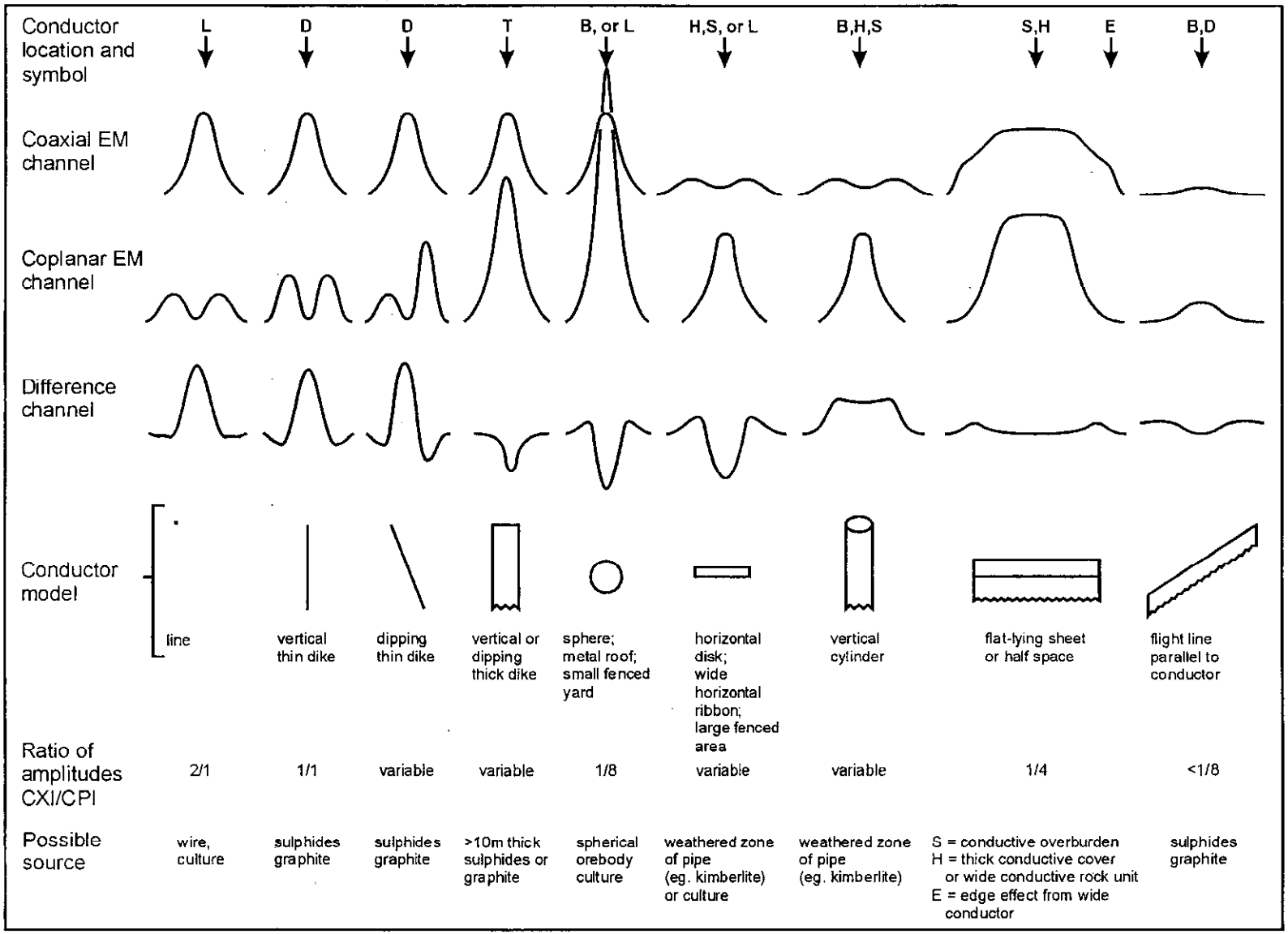

Typical DIGHEM anomaly shapes
Figure C-1

The attached EM anomaly list provides a tabulation of anomalies in ppm, conductance, and depth for the vertical sheet model. The EM anomaly list also shows the conductance and depth for a thin horizontal sheet (whole plane) model, but only the vertical sheet parameters appear on the EM map. The horizontal sheet model is suitable for a flatly dipping thin bedrock conductor such as a sulphide sheet having a thickness less than 10 m. The list also shows the resistivity and depth for a conductive earth (half-space) model, which is suitable for thicker slabs such as thick conductive overburden. In the EM anomaly list, a depth value of zero for the conductive earth model, in an area of thick cover, warns that the anomaly may be caused by conductive overburden.

Since discrete bodies normally are the targets of EM surveys, local base (or zero) levels are used to compute local anomaly amplitudes. This contrasts with the use of true zero levels which are used to compute true EM amplitudes. Local anomaly amplitudes are shown in the EM anomaly list and these are used to compute the vertical sheet parameters of conductance and depth. Not shown in the EM anomaly list are the true amplitudes which are used to compute the horizontal sheet and conductive earth parameters.

Questionable Anomalies

DIGHEM maps may contain EM responses which are displayed as asterisks (*). These responses denote weak anomalies of indeterminate conductance, which may reflect one

of the following: a weak conductor near the surface, a strong conductor at depth (e.g., 100 to 120 m below surface) or to one side of the flight line, or aerodynamic noise. Those responses which have the appearance of valid bedrock anomalies on the flight profiles are indicated by appropriate interpretive symbols (see EM legend on maps). The others probably do not warrant further investigation unless their locations are of considerable geological interest.

The Thickness Parameter

DIGHEM can provide an indication of the thickness of a steeply dipping conductor. The amplitude of the coplanar anomaly (e.g., CPI channel on the digital profile) increases relative to the coaxial anomaly (e.g., CXI) as the apparent thickness increases, i.e., the thickness in the horizontal plane. (The thickness is equal to the conductor width if the conductor dips at 90 degrees and strikes at right angles to the flight line.) This report refers to a conductor as thin when the thickness is likely to be less than 3 m, and thick when in excess of 10 m. Thick conductors are indicated on the EM map by parentheses "( )". For base metal exploration in steeply dipping geology, thick conductors can be high priority targets because many massive sulphide ore bodies are thick, whereas non-economic bedrock conductors are often thin. The system cannot sense the thickness when the strike of the conductor is subparallel to the flight line, when the conductor has a shallow dip, when the anomaly amplitudes are small, or when the resistivity of the environment is below 100 ohm-m.

Resistivity Mapping

Resistivity mapping is useful in areas where broad or flat lying conductive units are of interest. One example of this is the clay alteration which is associated with Carlin-type deposits in the south west United States. The Dighem system was able to identify the clay alteration zone over the Cove deposit. The alteration zone appeared as a strong resistivity low on the 900 Hz resistivity parameter. The 7,200 Hz and 56,000 Hz resistivities show more of the detail in the covering sediments, and delineate a range front fault. This is typical in many areas of the south west United States, where conductive near surface sediments, which may sometimes be alkalic, attenuate the higher frequencies.

Resistivity mapping has proven successful for locating diatremes in diamond exploration. Weathering products from relatively soft kimberlite pipes produce a resistivity contrast with the unaltered host rock. In many cases weathered kimberlite pipes were associated with thick conductive layers which contrasted with overlying or adjacent relatively thin layers of lake bottom sediments or overburden.

Areas of widespread conductivity are commonly encountered during surveys. These conductive zones may reflect alteration zones, shallow-dipping sulphide or graphite-rich units or conductive overburden. In such areas, anomalies can be generated by decreases of only 5 m in survey altitude as well as by increases in conductivity. The typical flight record in conductive areas is characterized by in-phase and quadrature channels which

are continuously active. Local EM peaks reflect either increases in conductivity of the earth or decreases in survey altitude. For such conductive areas, apparent resistivity profiles and contour maps are necessary for the correct interpretation of the airborne data. The advantage of the resistivity parameter is that anomalies caused by altitude changes are virtually eliminated, so the resistivity data reflect only those anomalies caused by conductivity changes. The resistivity analysis also helps the interpreter to differentiate between conductive bedrock and conductive overburden. For example, discrete conductors will generally appear as narrow lows on the contour map and broad conductors (e.g., overburden) will appear as wide lows.

The apparent resistivity is calculated using the pseudo-layer (or buried) half-space model defined by Fraser (1978)[6]. This model consists of a resistive layer overlying a conductive half-space. The depth channels give the apparent depth below surface of the conductive material. The apparent depth is simply the apparent thickness of the overlying resistive layer. The apparent depth (or thickness) parameter will be positive when the upper layer is more resistive than the underlying material, in which case the apparent depth may be quite close to the true depth.

The apparent depth will be negative when the upper layer is more conductive than the underlying material, and will be zero when a homogeneous half-space exists. The

---

[6] Resistivity mapping with an airborne multicoil electromagnetic system: Geophysics, v. 43, p.144-172

apparent depth parameter must be interpreted cautiously because it will contain any errors which may exist in the measured altitude of the EM bird (e.g., as caused by a dense tree cover). The inputs to the resistivity algorithm are the in-phase and quadrature components of the coplanar coil-pair. The outputs are the apparent resistivity of the conductive half-space (the source) and the sensor-source distance. The flying height is not an input variable, and the output resistivity and sensor-source distance are independent of the flying height when the conductivity of the measured material is sufficient to yield significant in-phase as well as quadrature responses. The apparent depth, discussed above, is simply the sensor-source distance minus the measured altitude or flying height. Consequently, errors in the measured altitude will affect the apparent depth parameter but not the apparent resistivity parameter.

The apparent depth parameter is a useful indicator of simple layering in areas lacking a heavy tree cover. The DIGHEM system has been flown for purposes of permafrost mapping, where positive apparent depths were used as a measure of permafrost thickness. However, little quantitative use has been made of negative apparent depths because the absolute value of the negative depth is not a measure of the thickness of the conductive upper layer and, therefore, is not meaningful physically. Qualitatively, a negative apparent depth estimate usually shows that the EM anomaly is caused by conductive overburden. Consequently, the apparent depth channel can be of significant help in distinguishing between overburden and bedrock conductors.

Interpretation in Conductive Environments

Environments having low background resistivities (e.g., below 30 ohm-m for a 900 Hz system) yield very large responses from the conductive ground. This usually prohibits the recognition of discrete bedrock conductors. However, DIGHEM data processing techniques produce three parameters which contribute significantly to the recognition of bedrock conductors in conductive environments. These are the in-phase and quadrature difference channels (DIFI and DIFQ, which are available only on systems with common frequencies on orthogonal coil pairs), and the resistivity and depth channels (RES and DP) for each coplanar frequency.

The EM difference channels (DIFI and DIFQ) eliminate most of the responses from conductive ground, leaving responses from bedrock conductors, cultural features (e.g., telephone lines, fences, etc.) and edge effects. Edge effects often occur near the perimeter of broad conductive zones. This can be a source of geologic noise. While edge effects yield anomalies on the EM difference channels, they do not produce resistivity anomalies. Consequently, the resistivity channel aids in eliminating anomalies due to edge effects. On the other hand, resistivity anomalies will coincide with the most highly conductive sections of conductive ground, and this is another source of geologic noise. The recognition of a bedrock conductor in a conductive environment therefore is based on the anomalous responses of the two difference channels (DIFI and DIFQ) and the

resistivity channels (RES). The most favourable situation is where anomalies coincide on all channels.

The DP channels, which give the apparent depth to the conductive material, also help to determine whether a conductive response arises from surficial material or from a conductive zone in the bedrock. When these channels ride above the zero level on the digital profiles (i.e., depth is negative), it implies that the EM and resistivity profiles are responding primarily to a conductive upper layer, i.e., conductive overburden. If the DP channels are below the zero level, it indicates that a resistive upper layer exists, and this usually implies the existence of a bedrock conductor. If the low frequency DP channel is below the zero level and the high frequency DP is above, this suggests that a bedrock conductor occurs beneath conductive cover.

Reduction of Geologic Noise

Geologic noise refers to unwanted geophysical responses. For purposes of airborne EM surveying, geologic noise refers to EM responses caused by conductive overburden and magnetic permeability. It was mentioned previously that the EM difference channels (i.e., channel DIFI for in-phase and DIFQ for quadrature) tend to eliminate the response of conductive overburden.

Magnetite produces a form of geological noise on the in-phase channels of all EM systems. Rocks containing less than 1% magnetite can yield negative in-phase anomalies caused by magnetic permeability. When magnetite is widely distributed throughout a survey area, the in-phase EM channels may continuously rise and fall, reflecting variations in the magnetite percentage, flying height, and overburden thickness. This can lead to difficulties in recognizing deeply buried bedrock conductors, particularly if conductive overburden also exists. However, the response of broadly distributed magnetite generally vanishes on the in-phase difference channel DIFI. This feature can be a significant aid in the recognition of conductors which occur in rocks containing accessory magnetite.

EM Magnetite Mapping

The information content of DIGHEM data consists of a combination of conductive eddy current responses and magnetic permeability responses. The secondary field resulting from conductive eddy current flow is frequency-dependent and consists of both in-phase and quadrature components, which are positive in sign. On the other hand, the secondary field resulting from magnetic permeability is independent of frequency and consists of only an in-phase component which is negative in sign. When magnetic permeability manifests itself by decreasing the measured amount of positive in-phase, its presence may be difficult to recognize. However, when it manifests itself by yielding a negative in-phase anomaly (e.g., in the absence of eddy current flow), its presence is assured. In this latter case, the negative component can be used to estimate the percent magnetite content.

A magnetite mapping technique was developed for the coplanar coil-pair of DIGHEM. The method can be complementary to magnetometer mapping in certain cases. Compared to magnetometry, it is far less sensitive but is more able to resolve closely spaced magnetite zones, as well as providing an estimate of the amount of magnetite in the rock. The method is sensitive to 1/4% magnetite by weight when the EM sensor is at a height of 30 m above a magnetitic half-space. It can individually resolve steep dipping narrow magnetite-rich bands which are separated by 60 m. Unlike magnetometry, the EM magnetite method is unaffected by remanent magnetism or magnetic latitude.

The EM magnetite mapping technique provides estimates of magnetite content which are usually correct within a factor of 2 when the magnetite is fairly uniformly distributed. EM magnetite maps can be generated when magnetic permeability is evident as negative in-phase responses on the data profiles.

Like magnetometry, the EM magnetite method maps only bedrock features, provided that the overburden is characterized by a general lack of magnetite. This contrasts with resistivity mapping which portrays the combined effect of bedrock and overburden.

Recognition of Culture

Cultural responses include all EM anomalies caused by man-made metallic objects. Such anomalies may be caused by inductive coupling or current gathering. The concern of the

interpreter is to recognize when an EM response is due to culture. Points of consideration used by the interpreter, when coaxial and coplanar coil-pairs are operated at a common frequency, are as follows:

1. Channels CXP and CPP monitor 60 Hz radiation. An anomaly on these channels shows that the conductor is radiating power. Such an indication is normally a guarantee that the conductor is cultural. However, care must be taken to ensure that the conductor is not a geologic body which strikes across a power line, carrying leakage currents.

2. A flight which crosses a "line" (e.g., fence, telephone line, etc.) yields a centre-peaked coaxial anomaly and an m-shaped coplanar anomaly.[7] When the flight crosses the cultural line at a high angle of intersection, the amplitude ratio of coaxial/coplanar response is 8. Such an EM anomaly can only be caused by a line. The geologic body which yields anomalies most closely resembling a line is the vertically dipping thin dike. Such a body, however, yields an amplitude ratio of 4 rather than 8. Consequently, an m-shaped coplanar anomaly with a CXI/CPI amplitude ratio of 8 is virtually a guarantee that the source is a cultural line.

3. A flight which crosses a sphere or horizontal disk yields centre-peaked coaxial and coplanar anomalies with a CXI/CPI amplitude ratio (i.e., coaxial/coplanar) of 1/8.

---

[7] See Figure C-1 presented earlier.

In the absence of geologic bodies of this geometry, the most likely conductor is a metal roof or small fenced yard.[8] Anomalies of this type are virtually certain to be cultural if they occur in an area of culture.

4. A flight which crosses a horizontal rectangular body or wide ribbon yields an m-shaped coaxial anomaly and a centre-peaked coplanar anomaly. In the absence of geologic bodies of this geometry, the most likely conductor is a large fenced area.[5] Anomalies of this type are virtually certain to be cultural if they occur in an area of culture.

5. EM anomalies which coincide with culture, as seen on the camera film or video display, are usually caused by culture. However, care is taken with such coincidences because a geologic conductor could occur beneath a fence, for example. In this example, the fence would be expected to yield an m-shaped coplanar anomaly as in case #2 above. If, instead, a centre-peaked coplanar anomaly occurred, there would be concern that a thick geologic conductor coincided with the cultural line.

6. The above description of anomaly shapes is valid when the culture is not conductively coupled to the environment. In this case, the anomalies arise from

---

[8] It is a characteristic of EM that geometrically similar anomalies are obtained from: (1) a planar conductor, and (2) a wire which forms a loop having dimensions identical to the perimeter of the equivalent planar conductor.

inductive coupling to the EM transmitter. However, when the environment is quite conductive (e.g., less than 100 ohm-m at 900 Hz), the cultural conductor may be conductively coupled to the environment. In this latter case, the anomaly shapes tend to be governed by current gathering. Current gathering can completely distort the anomaly shapes, thereby complicating the identification of cultural anomalies. In such circumstances, the interpreter can only rely on the radiation channels and on the camera film or video records.

Magnetics

Total field magnetics provides information on the magnetic properties of the earth materials in the survey area. The information can be used to locate magnetic bodies of direct interest for exploration, and for structural and lithological mapping.

The total field magnetic response reflects the abundance of magnetic material, in the source. Magnetite is the most common magnetic mineral. Other minerals such as ilmenite, pyrrhotite, franklinite, chromite, hematite, arsenopyrite, limonite and pyrite are also magnetic, but to a lesser extent than magnetite on average.

In some geological environments, an EM anomaly with magnetic correlation has a greater likelihood of being produced by sulphides than one which is non-magnetic. However,

sulphide ore bodies may be non-magnetic (e.g., the Kidd Creek deposit near Timmins, Canada) as well as magnetic (e.g., the Mattabi deposit near Sturgeon Lake, Canada).

Iron ore deposits will be anomalously magnetic in comparison to surrounding rock due to the concentration of iron minerals such as magnetite, ilmenite and hematite.

Changes in magnetic susceptibility often allow rock units to be differentiated based on the total field magnetic response. Geophysical classifications may differ from geological classifications if various magnetite levels exist within one general geological classification. Geometric considerations of the source such as shape, dip and depth, inclination of the earth's field and remanent magnetization will complicate such an analysis.

In general, mafic lithologies contain more magnetite and are therefore more magnetic than many sediments which tend to be weakly magnetic. Metamorphism and alteration can also increase or decrease the magnetization of a rock unit.

Textural differences on a total field magnetic contour, colour or shadow map due to the frequency of activity of the magnetic parameter resulting from inhomogeneities in the distribution of magnetite within the rock, may define certain lithologies. For example, near surface volcanics may display highly complex contour patterns with little line-to-line correlation.

Rock units may be differentiated based on the plan shapes of their total field magnetic responses. Mafic intrusive plugs can appear as isolated "bulls-eye" anomalies. Granitic intrusives appear as sub-circular zones, and may have contrasting rings due to contact metamorphism. Generally, granitic terrain will lack a pronounced strike direction, although granite gneiss may display strike.

Linear north-south units are theoretically not well-defined on total field magnetic maps in equatorial regions due to the low inclination of the earth's magnetic field. However, most stratigraphic units will have variations in composition along strike which will cause the units to appear as a series of alternating magnetic highs and lows.

Faults and shear zones may be characterized by alteration which causes destruction of magnetite (e.g., weathering) which produces a contrast with surrounding rock. Structural breaks may be filled by magnetite-rich, fracture filling material as is the case with diabase dikes, or by non-magnetic felsic material.

Faulting can also be identified by patterns in the magnetic total field contours or colours. Faults and dikes tend to appear as lineaments and often have strike lengths of several kilometres. Offsets in narrow, magnetic, stratigraphic trends also delineate structure. Sharp contrasts in magnetic lithologies may arise due to large displacements along strike-slip or dip-slip faults.

Radiometrics

Radioelement concentrations are measures of the abundance of radioactive elements in the rock. The original abundance of the radioelements in any rock can be altered by the subsequent processes of metamorphism and weathering.

Gamma radiation in the range which is measured in the thorium, potassium, uranium and total count windows is strongly attenuated by rock, overburden and water. Almost all of the total radiation measured from rock and overburden originates in the upper .5 metres. Moisture in soil and bodies of water will mask the radioactivity from underlying rock. Weathered rock materials which have been displaced by glacial, water or wind action will not reflect the general composition of the underlying bedrock. Where residual soils exist, they may reflect the composition of underlying rock except where equilibrium does not exist between the original radioelement and the products in its decay series.

Radioelement counts (expressed as counts per second) are the rates of detection of the gamma radiation from specific decaying particles corresponding to products in each radioelements decay series. The radiation source for uranium is bismuth (Bi-214), for thorium it is thallium (Tl-208) and for potassium it is potassium (K-40).

The uranium and thorium radioelement concentrations are dependent on a state of equilibrium between the parent and daughter products in the decay series. Some

daughter products in the uranium decay are long lived and could be removed by processes such as leaching. One product in the series, radon (Rn-222), is a gas which can easily escape. Both of these factors can affect the degree to which the calculated uranium concentrations reflect the actual composition of the source rock. Because the daughter products of thorium are relatively short lived, there is more likelihood that the thorium decay series is in equilibrium.

Lithological discrimination can be based on the measured relative concentrations and total, combined, radioactivity of the radioelements. Feldspar and mica contain potassium. Zircon, sphene and apatite are accessory minerals in igneous rocks which are sources of uranium and thorium. Monazite, thorianite, thorite, uraninite and uranothorite are also sources of uranium and thorium which are found in granites and pegmatites.

In general, the abundance of uranium, thorium and potassium in igneous rock increases with acidity. Pegmatites commonly have elevated concentrations of uranium relative to thorium. Sedimentary rocks derived from igneous rocks may have characteristic signatures which are influenced by their parent rocks, but these will have been altered by subsequent weathering and alteration.

Metamorphism and alteration will cause variations in the abundance of certain radioelements relative to each other. For example, alterative processes may cause uranium enrichment to the extent that a rock will be of economic interest. Uranium anomalies are more likely to be economically significant if they consist of an increase in

the uranium relative to thorium and potassium, rather than a sympathetic increase in all three radioelements.

Faults can exhibit radioactive highs due to increased permeability which allows radon migration, or as lows due to structural control of drainage and fluvial sediments which attenuate gamma radiation from the underlying rocks. Faults can also be recognized by sharp contrasts in radiometric lithologies due to large strike-slip or dip-slip displacements. Changes in relative radioelement concentrations due to alteration will also define faults.

Similar to magnetics, certain rock types can be identified by their plan shapes if they also produce a radiometric contrast with surrounding rock. For example, granite intrusions will appear as sub-circular bodies, and may display concentric zonations. They will tend to lack a prominent strike direction. Offsets of narrow, continuous, stratigraphic units with contrasting radiometric signatures can identify faulting, and folding of stratigraphic trends will also be apparent.

APPENDIX D

EM ANOMALY LIST

EM Anomaly List

Label	Fid	Interp	XUTM m	YUTM m	CX 5500 HZ Real ppm	CX 5500 HZ Quad ppm	CP 7200 HZ Real ppm	CP 7200 HZ Quad ppm	CP 900 HZ Real ppm	CP 900 HZ Quad ppm	Vertical Dike COND siemens	Vertical Dike DEPTH* m	Mag. Corr NT
LINE 10010			FLIGHT 17										
A	2018.9	S?	687514	6265166	12.9	7.1	70.9	24.7	85.4	3.8	---	---	71
B	2003.8	S?	687686	6265154	2.0	3.8	2.3	28.1	2.0	3.3	---	---	15
C	1943.4	S	689156	6265145	7.4	15.1	6.5	63.5	3.4	8.9	0.6	18	0
LINE 10012			FLIGHT 17										
A	2414.3	S?	683612	6265169	9.1	9.7	78.1	38.3	92.9	6.3	---	---	214
B	2382.3	S	684541	6265146	11.7	8.3	39.7	30.4	43.6	5.0	---	---	0
LINE 10013			FLIGHT 17										
A	2934.8	S?	680293	6265162	2.9	4.5	4.3	26.6	1.1	4.5	---	---	0
B	2899.1	S?	681252	6265169	0.5	6.2	15.8	26.0	19.7	4.4	---	---	33
C	2862.4	S	682184	6265138	2.1	6.1	34.3	22.9	26.4	4.5	---	---	0
D	2845.5	S?	682416	6265144	0.0	2.7	78.9	32.0	0.0	6.2	---	---	151
E	2826.0	S?	682593	6265117	0.0	3.9	28.7	15.5	27.9	4.1	---	---	0
LINE 10020			FLIGHT 17										
A	3264.0	S?	680254	6264951	0.7	6.8	6.9	19.5	9.2	3.6	---	---	132
B	3278.6	S?	680618	6264947	0.2	6.0	6.2	17.9	15.1	1.7	---	---	177
C	3322.6	S?	682125	6264945	6.4	1.6	14.4	18.2	13.2	5.1	---	---	143
LINE 10021			FLIGHT 17										
A	3489.8	S?	683029	6264941	2.1	2.6	8.1	12.3	10.7	2.1	---	---	0
B	3514.5	S?	683494	6264978	6.8	8.1	44.1	62.5	49.3	9.7	0.9	29	0
LINE 10022			FLIGHT 17										
A	3646.0	S?	685496	6264955	5.4	14.1	29.9	39.5	33.5	7.9	---	---	0
B	3661.2	S	685746	6264962	9.1	12.1	97.0	37.7	116.3	6.6	---	---	0

CX = COAXIAL
CP = COPLANAR

Note:EM values shown above are local amplitudes

*Estimated Depth may be unreliable because the stronger part of the conductor may be deeper or to one side of the flight line, or because of a shallow dip or magnetite/overburden effects

EM Anomaly List

Label	Fid	Interp	XUTM m	YUTM m	CX 5500 HZ Real ppm	CX 5500 HZ Quad ppm	CP 7200 HZ Real ppm	CP 7200 HZ Quad ppm	CP 900 HZ Real ppm	CP 900 HZ Quad ppm	Vertical Dike COND siemens	Vertical Dike DEPTH* m	Mag. Corr NT
LINE 10050			FLIGHT 17										
A	5712.8	S?	687730	6264338	1.2	15.1	3.1	54.1	2.3	7.7	---	---	147
LINE 10051			FLIGHT 17										
A	6041.2	S	682767	6264353	5.8	0.2	21.9	8.2	26.4	1.6	---	---	0
B	6032.0	S?	682937	6264357	0.8	7.5	26.9	19.4	18.2	3.4	---	---	94
C	6010.1	S	683404	6264351	4.1	2.2	24.2	14.6	27.2	2.4	---	---	0
D	6000.2	S	683656	6264339	4.6	2.8	9.3	28.0	13.9	4.6	---	---	146
E	5926.7	S?	685227	6264369	4.8	6.2	13.0	24.5	17.7	3.0	0.7	25	0
F	5918.5	S	685463	6264342	3.5	6.1	6.2	39.9	0.0	6.3	---	---	0
G	5909.2	S	685625	6264331	3.7	0.1	20.6	0.8	17.0	0.5	---	---	20
H	5898.1	S	685808	6264342	2.7	3.5	3.8	32.1	3.3	5.3	---	---	0
I	5879.9	S	686092	6264372	3.9	5.6	11.2	26.5	10.9	4.6	0.6	40	0
LINE 10052			FLIGHT 17										
A	6268.1	B?	679904	6264359	1.1	2.4	7.1	10.6	3.7	2.0	---	---	0
LINE 10060			FLIGHT 17										
A	6574.2	S?	681190	6264132	0.0	9.4	0.2	65.2	1.1	8.9	---	---	105
B	6602.0	S?	681946	6264154	4.2	3.8	17.0	18.3	18.2	2.5	1.1	43	0
C	6680.7	S?	684600	6264128	1.4	14.0	0.3	91.7	0.0	13.6	---	---	0
D	6893.4	S?	686956	6264156	2.8	1.8	4.3	16.0	0.0	2.1	---	---	73
LINE 10070			FLIGHT 17										
A	7528.0	S	680235	6263944	0.9	8.0	6.6	45.1	0.3	6.8	---	---	0
B	7287.8	S	685582	6263946	6.4	7.2	15.5	44.1	16.9	7.9	1.0	27	45
C	7281.6	S	685716	6263953	3.9	12.0	15.1	45.7	16.9	7.2	---	---	0
D	7240.8	S	686466	6263953	3.2	0.2	10.5	13.8	6.8	2.6	---	---	572

CX = COAXIAL
CP = COPLANAR

Note:EM values shown above are local amplitudes

*Estimated Depth may be unreliable because the stronger part of the conductor may be deeper or to one side of the flight line, or because of a shallow dip or magnetite/overburden effects

EM Anomaly List

Label	Fid	Interp	XUTM m	YUTM m	CX 5500 HZ Real ppm	CX 5500 HZ Quad ppm	CP 7200 HZ Real ppm	CP 7200 HZ Quad ppm	CP 900 HZ Real ppm	CP 900 HZ Quad ppm	Vertical Dike COND siemens	Vertical Dike DEPTH* m	Mag. Corr NT
LINE 10090			FLIGHT 18										
F	918.8	S	688008	6263559	3.4	8.0	9.2	18.7	12.2	3.5	---	---	0
G	845.8	S?	689424	6263538	0.0	8.1	7.6	22.9	18.8	3.8	---	---	0
LINE 10091			FLIGHT 18										
A	1516.7	S	679554	6263519	3.1	9.3	18.6	34.1	24.4	4.2	---	---	0
B	1505.0	S?	679956	6263533	5.9	22.3	23.9	75.7	25.1	11.1	---	---	0
C	1502.3	S?	680056	6263544	7.8	22.3	23.9	75.7	25.1	11.1	---	---	151
D	1498.0	S?	680215	6263550	7.8	11.3	23.9	38.7	3.7	6.8	---	---	154
LINE 10100			FLIGHT 18										
A	1584.0	S?	680268	6263347	0.0	7.0	28.1	28.4	31.0	4.3	---	---	59
B	1788.7	S?	684946	6263328	3.7	6.2	22.1	26.1	26.5	3.6	0.5	35	0
C	1803.6	S?	685157	6263342	9.9	13.1	0.6	59.7	0.0	8.9	---	---	0
D	1807.7	S	685218	6263344	12.3	14.4	25.3	59.7	29.9	8.9	---	---	0
E	1816.9	S?	685454	6263339	11.3	17.4	68.3	85.4	64.7	12.4	0.8	20	0
F	1927.4	S	686324	6263332	1.3	1.8	19.8	14.7	17.5	2.0	---	---	0
G	1929.9	S?	686346	6263331	2.4	1.2	9.6	15.4	10.4	2.8	---	---	0
H	1947.2	S?	686536	6263344	8.1	1.6	32.9	25.9	34.9	4.1	---	---	0
I	2119.7	S	689170	6263348	4.3	8.5	13.4	31.0	13.9	5.1	0.5	24	0
LINE 10110			FLIGHT 18										
A	2212.3	S?	688428	6263162	6.7	6.5	14.6	36.9	15.2	6.9	---	---	0
B	2179.8	S?	689209	6263141	16.8	6.4	61.1	42.9	69.7	6.6	---	---	242
C	2165.4	S?	689457	6263140	6.5	4.2	28.1	26.0	22.5	3.7	1.9	48	0
LINE 10111			FLIGHT 18										
A	2619.9	S?	681749	6263140	0.0	4.0	18.9	15.6	23.1	3.7	---	---	787
B	2494.7	S?	685446	6263144	17.7	26.8	73.2	102.2	91.0	16.0	---	---	465

CX = COAXIAL
CP = COPLANAR

Note:EM values shown above are local amplitudes

*Estimated Depth may be unreliable because the stronger part of the conductor may be deeper or to one side of the flight line, or because of a shallow dip or magnetite/overburden effects

EM Anomaly List

Label	Fid	Interp	XUTM m	YUTM m	CX 5500 HZ Real ppm	CX 5500 HZ Quad ppm	CP 7200 HZ Real ppm	CP 7200 HZ Quad ppm	CP 900 HZ Real ppm	CP 900 HZ Quad ppm	Vertical Dike COND siemens	Vertical Dike DEPTH* m	Mag. Corr NT
LINE 10130			FLIGHT 19										
C	529.4	S?	681039	6262749	37.1	8.6	181.0	19.0	237.8	0.7	---	---	0
D	564.1	S?	681311	6262747	1.3	2.0	4.1	14.9	2.0	1.9	---	---	26
E	574.8	S?	681596	6262744	1.9	3.7	22.4	13.9	26.0	2.6	---	---	0
LINE 10131			FLIGHT 19										
A	705.9	S?	683489	6262736	4.7	3.8	133.0	27.1	18.5	4.3	1.3	48	0
B	744.2	S?	684840	6262749	8.1	17.8	27.0	99.8	10.9	14.8	---	---	0
C	752.1	S	685133	6262734	0.0	3.7	24.3	25.7	12.5	4.0	---	---	56
D	767.1	S?	685405	6262750	0.0	14.7	28.2	64.3	26.5	10.3	---	---	0
LINE 10135			FLIGHT 19										
A	1157.1	S?	687711	6262741	8.6	7.8	60.9	36.9	72.0	5.3	---	---	258
LINE 10136			FLIGHT 19										
A	1241.2	S	688345	6262740	2.3	3.9	3.6	20.1	1.4	2.4	---	---	0
B	1276.6	S	689021	6262759	7.8	2.9	7.3	14.0	7.0	3.1	---	---	0
LINE 10141			FLIGHT 19										
A	1913.5	S	684099	6262547	1.2	7.9	86.8	14.5	97.5	2.2	---	---	0
B	1877.8	S?	684850	6262549	2.3	9.9	80.3	87.4	66.1	12.3	---	---	0
C	1873.8	S	685004	6262556	4.3	19.1	80.3	87.4	54.9	14.2	---	---	0
D	1861.5	S?	685433	6262545	3.3	5.8	31.0	26.7	29.8	4.7	0.5	18	0
E	1836.0	S?	685903	6262533	0.0	4.1	64.3	29.6	77.3	4.8	---	---	495
F	1698.5	S?	687756	6262542	0.1	9.2	10.3	25.3	10.6	3.9	---	---	476
G	1647.7	S?	688282	6262546	0.0	7.7	1.6	12.8	3.0	2.4	---	---	169
LINE 10143			FLIGHT 19										
A	2352.7	S?	679707	6262583	0.5	5.3	5.0	26.1	6.3	4.5	---	---	0

CX = COAXIAL
CP = COPLANAR

Note:EM values shown above are local amplitudes

*Estimated Depth may be unreliable because the stronger part of the conductor may be deeper or to one side of the flight line, or because of a shallow dip or magnetite/overburden effects

EM Anomaly List

Label	Fid	Interp	XUTM m	YUTM m	CX 5500 HZ Real ppm	CX 5500 HZ Quad ppm	CP 7200 HZ Real ppm	CP 7200 HZ Quad ppm	CP 900 HZ Real ppm	CP 900 HZ Quad ppm	Vertical Dike COND siemens	Vertical Dike DEPTH* m	Mag. Corr NT
LINE	10154		FLIGHT 19										
A	3208.0	S	687562	6262351	33.7	7.0	177.8	44.1	201.5	6.7	15.4	28	0
B	3215.8	S	687714	6262365	6.5	10.2	186.0	44.3	214.1	5.7	---	---	0
C	3266.1	S	688396	6262349	3.6	3.5	31.2	9.7	37.9	0.7	1.0	33	0
D	3283.8	S	688896	6262348	3.9	7.5	13.8	30.5	17.7	4.5	---	---	0
E	3311.3	S	689407	6262336	3.4	4.8	7.8	24.0	8.0	3.1	0.6	40	0
LINE	10160		FLIGHT 19										
A	3463.9	S?	687745	6262129	22.8	11.2	42.2	37.9	54.7	6.1	4.1	15	0
B	3451.9	S	687985	6262128	0.0	10.9	23.1	45.9	30.8	8.4	---	---	0
C	3440.0	S	688206	6262134	2.9	2.7	18.6	6.6	31.5	2.0	---	---	0
D	3430.5	S	688472	6262159	8.1	11.1	48.3	70.2	54.0	11.5	---	---	0
E	3428.0	S?	688545	6262157	8.6	19.3	48.3	70.2	54.0	11.5	0.6	17	0
F	3416.1	S?	688773	6262140	0.0	17.9	55.0	51.5	65.3	8.3	---	---	73
G	3401.7	S	688975	6262150	4.7	12.6	64.7	28.0	72.0	3.2	---	---	16
H	3371.9	S?	689278	6262142	13.3	3.2	57.3	47.6	61.9	7.4	---	---	52
LINE	10161		FLIGHT 19										
A	3876.4	S?	682520	6262146	28.2	5.1	175.1	61.1	205.6	9.0	---	---	0
B	3855.4	S	683129	6262157	6.5	6.3	52.5	30.4	8.7	5.2	---	---	724
C	3799.8	S	684101	6262142	0.2	11.3	21.8	31.1	3.1	4.8	---	---	0
D	3730.1	S?	685120	6262154	0.0	12.4	33.8	59.4	48.4	10.1	---	---	777
E	3723.4	S	685372	6262136	5.0	10.8	22.1	62.8	5.9	11.0	0.5	12	123
F	3703.9	S?	685898	6262141	0.0	3.9	89.2	21.9	104.4	5.0	---	---	868
LINE	10162		FLIGHT 19										
A	4241.9	S?	679386	6262139	2.1	6.2	27.2	15.0	31.2	2.3	---	---	0
B	4189.0	S	680288	6262157	12.3	7.4	27.7	26.0	57.4	4.0	---	---	65

CX = COAXIAL
CP = COPLANAR

Note:EM values shown above are local amplitudes

*Estimated Depth may be unreliable because the stronger part of the conductor may be deeper or to one side of the flight line, or because of a shallow dip or magnetite/overburden effects

EM Anomaly List

Label	Fid	Interp	XUTM m	YUTM m	CX 5500 HZ Real ppm	CX 5500 HZ Quad ppm	CP 7200 HZ Real ppm	CP 7200 HZ Quad ppm	CP 900 HZ Real ppm	CP 900 HZ Quad ppm	Vertical Dike COND siemens	Vertical Dike DEPTH* m	Mag. Corr NT
LINE	10182		FLIGHT 20										
B	754.8	S?	682348	6261713	12.9	1.2	0.0	18.2	0.0	3.6	---	---	0
C	768.4	S	682873	6261801	1.2	10.1	104.9	41.4	124.0	7.0	---	---	169
D	775.4	S	683178	6261770	2.7	3.3	112.0	6.0	126.8	1.2	---	---	0
E	785.6	S	683615	6261739	3.5	10.3	22.9	24.1	0.6	4.4	---	---	0
F	798.8	S?	684121	6261748	4.3	8.0	42.7	45.6	30.4	7.4	---	---	0
G	830.3	S?	684757	6261756	32.7	7.5	126.2	54.4	152.1	6.8	---	---	0
H	832.9	S?	684811	6261757	30.0	4.7	143.2	54.4	171.4	6.8	---	---	0
I	853.8	S?	685249	6261758	12.5	11.0	143.7	39.9	163.2	7.4	---	---	0
J	862.3	S?	685565	6261766	0.0	24.9	63.1	140.0	41.3	22.8	---	---	182
K	873.8	S	685878	6261749	0.0	7.3	29.9	41.7	40.1	6.2	---	---	0
LINE	10183		FLIGHT 20										
A	1053.0	S	687036	6261754	17.0	2.0	67.8	32.5	76.3	5.6	---	---	0
B	1055.9	S	687103	6261754	27.4	8.0	67.8	32.5	76.3	5.6	8.9	18	0
LINE	10184		FLIGHT 20										
A	1147.8	S?	687828	6261746	3.8	4.4	56.3	26.8	66.0	3.7	0.8	42	262
B	1155.8	S?	687972	6261761	3.7	0.0	11.4	15.4	13.4	1.9	---	---	38
C	1173.2	S?	688442	6261741	3.9	18.0	8.4	58.6	8.8	8.8	---	---	124
D	1184.6	B?	688669	6261741	3.3	1.4	11.7	45.0	13.4	7.1	---	---	0
LINE	10185		FLIGHT 20										
A	1296.0	S?	689436	6261747	0.4	4.4	13.3	18.9	2.9	3.7	---	---	29
LINE	10190		FLIGHT 20										
A	1641.3	S?	684143	6261538	8.2	1.6	114.9	30.1	134.4	1.3	---	---	0
B	1603.2	S	684938	6261545	3.6	1.5	12.6	10.8	15.0	1.4	---	---	0
C	1588.0	S	685156	6261545	1.3	1.8	181.9	15.0	211.7	1.3	---	---	0

CX = COAXIAL
CP = COPLANAR

Note:EM values shown above are local amplitudes

*Estimated Depth may be unreliable because the stronger part of the conductor may be deeper or to one side of the flight line, or because of a shallow dip or magnetite/overburden effects

EM Anomaly List

Label	Fid	Interp	XUTM m	YUTM m	CX 5500 HZ Real ppm	CX 5500 HZ Quad ppm	CP 7200 HZ Real ppm	CP 7200 HZ Quad ppm	CP 900 HZ Real ppm	CP 900 HZ Quad ppm	Vertical Dike COND siemens	Vertical Dike DEPTH* m	Mag. Corr NT
LINE	10210		FLIGHT 20										
A	3041.2	S?	684072	6261147	6.5	13.2	50.6	81.7	19.3	16.4	0.5	13	167
B	3033.5	S?	684237	6261147	4.1	25.1	45.6	138.6	14.4	21.5	0.2	0	0
C	2989.8	S?	685164	6261144	12.1	7.5	255.4	53.2	311.2	7.1	---	---	1611
D	2980.0	S?	685339	6261145	6.2	2.4	244.1	26.7	292.2	5.1	---	---	0
E	2960.1	S?	685752	6261151	3.8	13.1	27.2	52.6	30.0	8.0	---	---	0
F	2953.3	S?	685984	6261147	8.5	5.0	23.8	35.8	13.5	6.5	2.3	50	0
G	2882.2	S?	688380	6261144	11.1	12.6	18.3	44.2	30.8	7.5	---	---	34
LINE	10215		FLIGHT 20										
A	3443.8	S?	679636	6261140	5.8	13.9	10.6	50.9	7.2	9.0	---	---	0
B	3424.3	S	680234	6261145	1.7	11.0	9.3	23.2	11.0	4.0	---	---	0
LINE	10220		FLIGHT 20										
A	3487.7	S?	679618	6260965	5.4	13.0	14.2	56.9	9.9	8.9	---	---	0
B	3572.0	S	681135	6260946	2.5	5.6	2.6	29.0	3.4	3.6	---	---	0
C	3790.4	B	684040	6260956	7.2	5.9	46.2	30.3	195.3	1.5	---	---	0
D	3800.3	B?	684166	6260956	25.1	85.2	73.4	422.8	193.5	82.8	---	---	1067
E	3814.2	D	684472	6260942	14.7	18.3	45.2	104.5	10.3	20.8	1.1	18	106
F	3853.2	S	685735	6260950	21.8	6.7	151.0	11.9	176.6	2.0	---	---	0
G	3860.4	S?	686075	6260928	9.5	7.2	38.4	38.6	37.8	6.2	---	---	0
H	3914.3	S?	688364	6260943	3.5	1.1	14.4	15.9	16.3	1.9	---	---	48
I	3946.7	S?	689423	6260949	4.0	5.1	9.3	28.8	9.4	3.7	0.7	47	0
LINE	10230		FLIGHT 20										
A	4609.3	S?	680254	6260733	2.8	8.3	20.4	29.4	16.9	7.2	---	---	744
B	4536.1	S	681595	6260738	3.9	3.8	3.9	34.0	0.3	4.8	---	---	0
C	4519.7	S?	681782	6260750	39.9	0.0	223.8	13.6	271.3	1.1	---	---	0

CX = COAXIAL
CP = COPLANAR

Note:EM values shown above are local amplitudes

*Estimated Depth may be unreliable because the stronger part of the conductor may be deeper or to one side of the flight line, or because of a shallow dip or magnetite/overburden effects

EM Anomaly List

Label	Fid	Interp	XUTM m	YUTM m	CX 5500 HZ Real ppm	CX 5500 HZ Quad ppm	CP 7200 HZ Real ppm	CP 7200 HZ Quad ppm	CP 900 HZ Real ppm	CP 900 HZ Quad ppm	Vertical Dike COND siemens	Vertical Dike DEPTH* m	Mag. Corr NT
LINE 10251			FLIGHT 21										
B	1656.7	S	680149	6260341	1.2	8.6	25.0	7.5	23.2	1.7	---	---	0
C	1647.6	S?	680485	6260348	3.4	9.4	30.3	62.4	27.8	10.0	---	---	904
D	1582.0	S?	681691	6260339	2.2	4.1	22.7	29.6	4.2	4.8	---	---	0
LINE 10260			FLIGHT 21										
A	1745.0	S	679726	6260130	2.1	1.7	5.8	43.6	7.1	6.7	---	---	162
B	1768.8	S?	680410	6260133	1.6	8.6	18.9	44.8	11.1	9.1	---	---	0
C	1772.6	S?	680546	6260130	9.0	10.9	18.9	50.2	11.1	8.1	1.0	22	0
LINE 10263			FLIGHT 21										
A	2077.6	S?	682315	6260146	0.0	6.8	0.1	46.3	0.0	7.6	---	---	0
B	2142.0	S?	683748	6260154	3.9	3.0	14.2	16.1	19.3	2.9	1.2	54	20
C	2160.0	S?	684006	6260140	11.8	0.0	9.2	15.6	11.1	2.8	---	---	0
D	2184.5	S	684371	6260144	4.0	19.3	7.2	100.8	15.2	15.6	---	---	0
E	2204.4	S	684769	6260145	0.0	12.5	134.6	94.8	171.6	15.4	---	---	0
F	2218.8	S?	685238	6260142	9.4	3.5	30.5	24.2	28.0	4.3	4.3	42	0
G	2233.8	S	685908	6260143	3.4	1.5	5.8	10.3	6.8	2.5	---	---	253
H	2255.3	S	686784	6260142	1.8	5.5	11.1	18.5	8.3	2.9	---	---	0
LINE 10270			FLIGHT 21										
A	2534.2	S	684594	6259940	6.6	0.4	57.3	94.1	60.8	15.3	---	---	0
B	2526.7	S	684738	6259939	8.1	6.8	74.1	87.7	76.1	13.4	1.5	40	93
C	2454.3	S?	686786	6259930	3.7	8.1	33.3	19.9	36.2	2.9	---	---	0
D	2426.0	S?	687789	6259929	0.5	3.5	0.5	53.5	1.5	7.9	---	---	426
LINE 10271			FLIGHT 21										
A	2883.7	S?	679776	6259930	5.7	5.1	12.3	25.4	17.9	4.1	1.2	42	299
B	2852.3	S	680589	6259914	1.9	6.9	32.6	78.7	19.8	11.5	---	---	0

CX = COAXIAL
CP = COPLANAR

Note:EM values shown above are local amplitudes

*Estimated Depth may be unreliable because the stronger part of the conductor may be deeper or to one side of the flight line, or because of a shallow dip or magnetite/overburden effects

EM Anomaly List

Label	Fid	Interp	XUTM m	YUTM m	CX 5500 HZ Real ppm	CX 5500 HZ Quad ppm	CP 7200 HZ Real ppm	CP 7200 HZ Quad ppm	CP 900 HZ Real ppm	CP 900 HZ Quad ppm	Vertical Dike COND siemens	Vertical Dike DEPTH* m	Mag. Corr NT
LINE 10300			FLIGHT 21										
G	200.8	S?	686830	6259357	9.2	0.0	21.6	29.9	25.1	0.4	---	---	79
H	171.5	S?	687837	6259360	3.2	3.5	15.4	16.8	17.4	1.8	0.8	49	0
I	167.1	S	687995	6259357	4.9	3.6	11.1	15.3	14.9	2.4	1.5	56	190
J	141.6	S	688977	6259364	10.0	14.5	51.5	98.0	63.9	14.0	---	---	131
K	122.7	S?	689695	6259349	0.7	7.8	18.3	42.9	20.0	5.7	---	---	0
LINE 10310			FLIGHT 22										
A	2515.4	S?	680242	6259137	0.8	3.7	21.4	4.1	15.0	0.5	---	---	0
B	2465.7	S?	681320	6259140	30.3	20.7	122.8	82.4	151.1	11.5	---	---	0
C	2452.3	S	681789	6259146	3.9	6.8	6.7	69.5	7.1	10.6	---	---	0
D	2328.8	S?	686042	6259140	0.0	2.6	4.3	18.6	6.6	3.4	---	---	1208
E	2311.1	S?	686676	6259134	3.9	1.0	0.8	9.8	1.0	2.0	---	---	0
F	2304.8	S?	686899	6259123	2.9	0.8	9.9	13.9	6.4	2.1	---	---	15
G	2279.7	B?	687734	6259144	3.5	3.0	2.6	15.6	4.4	2.5	1.1	59	0
H	2243.2	S?	688941	6259145	1.9	1.2	15.1	14.7	14.3	2.9	---	---	0
I	2226.0	S?	689524	6259140	0.3	6.1	11.0	44.4	8.7	6.0	---	---	0
LINE 10320			FLIGHT 22										
A	2699.1	S?	680248	6258949	2.3	11.9	11.0	47.4	9.4	6.2	---	---	0
B	2745.6	S?	681121	6258954	2.6	0.5	23.8	18.0	27.0	3.2	---	---	0
C	2766.5	S?	681943	6258925	3.8	4.2	16.5	34.4	62.2	4.6	---	---	801
D	2886.4	S?	686663	6258937	1.9	2.0	23.0	13.7	26.4	2.5	---	---	0
E	2911.1	S?	687499	6258925	2.5	8.2	8.9	38.3	10.4	4.7	---	---	266
F	2956.0	S?	689231	6258942	1.8	1.9	4.5	7.1	40.5	1.6	---	---	899
LINE 10330			FLIGHT 22										
A	3359.5	S?	679653	6258748	0.0	9.6	2.5	33.7	1.1	4.1	---	---	26
B	3318.8	S?	680128	6258741	0.1	14.0	7.5	64.2	8.8	8.4	---	---	0

CX = COAXIAL
CP = COPLANAR

Note:EM values shown above are local amplitudes

*Estimated Depth may be unreliable because the stronger part of the conductor may be deeper or to one side of the flight line, or because of a shallow dip or magnetite/overburden effects

EM Anomaly List

Label	Fid	Interp	XUTM m	YUTM m	CX 5500 HZ Real ppm	CX 5500 HZ Quad ppm	CP 7200 HZ Real ppm	CP 7200 HZ Quad ppm	CP 900 HZ Real ppm	CP 900 HZ Quad ppm	Vertical Dike COND siemens	Vertical Dike DEPTH* m	Mag. Corr NT
LINE 10370			FLIGHT 22										
A	5471.9	S	680563	6257949	1.3	0.8	7.4	16.5	9.3	2.5	---	---	0
B	5461.9	S	680760	6257949	2.9	5.2	0.4	49.1	0.0	7.3	---	---	0
C	5441.8	S?	681349	6257953	1.8	7.0	9.8	21.7	14.0	3.5	---	---	0
D	5424.7	S	681892	6257952	12.5	3.4	60.1	13.3	105.4	2.0	7.4	42	0
E	5415.9	S?	682175	6257947	19.3	0.3	89.4	18.9	103.7	3.1	---	---	3108
F	5242.4	S	686617	6257946	0.9	8.8	2.9	43.2	2.3	6.2	---	---	0
G	5238.0	S	686711	6257940	4.0	0.6	3.3	33.5	0.8	5.7	---	---	0
LINE 10380			FLIGHT 23										
A	498.8	S?	679883	6257747	0.6	5.1	1.4	15.3	3.5	3.2	---	---	0
B	542.9	S	680524	6257748	3.8	2.8	8.1	31.5	4.1	5.0	---	---	0
C	593.3	S?	682007	6257736	0.5	5.0	44.3	18.7	51.6	3.8	---	---	0
D	865.1	S?	686840	6257775	5.3	6.0	6.3	49.9	4.3	6.8	---	---	0
LINE 10390			FLIGHT 23										
A	1178.3	S	689453	6257549	1.9	4.7	41.1	26.3	25.3	3.7	---	---	0
LINE 10392			FLIGHT 23										
A	1756.8	S?	680492	6257562	1.9	1.3	2.4	16.0	0.1	2.4	---	---	0
B	1751.2	S	680637	6257559	4.5	7.5	1.8	22.1	2.9	4.2	0.6	20	0
C	1694.1	S?	682254	6257558	11.2	3.4	34.9	6.9	37.6	1.8	6.3	41	0
D	1680.7	S	682629	6257556	6.5	0.4	32.1	19.3	33.8	2.7	---	---	884
E	1496.0	S	686493	6257556	0.0	2.7	0.2	24.4	0.0	3.5	---	---	14
F	1487.9	S	686719	6257559	3.2	0.9	11.2	17.3	10.5	2.2	---	---	0
LINE 10400			FLIGHT 23										
A	2200.1	S?	682487	6257340	6.9	1.4	18.0	8.1	17.5	1.7	---	---	0

CX = COAXIAL
CP = COPLANAR

Note:EM values shown above are local amplitudes

*Estimated Depth may be unreliable because the stronger part of the conductor may be deeper or to one side of the flight line, or because of a shallow dip or magnetite/overburden effects

EM Anomaly List

Label	Fid	Interp	XUTM m	YUTM m	CX 5500 HZ Real ppm	CX 5500 HZ Quad ppm	CP 7200 HZ Real ppm	CP 7200 HZ Quad ppm	CP 900 HZ Real ppm	CP 900 HZ Quad ppm	Vertical Dike COND siemens	Vertical Dike DEPTH* m	Mag. Corr NT
LINE	19020		FLIGHT 23										
B	4052.6	S?	688998	6263451	0.0	6.3	9.2	15.9	10.4	2.3	---	---	0
C	4012.9	S?	688985	6262431	3.3	1.2	2.3	12.1	0.6	1.9	---	---	0
D	3992.0	S?	689001	6262145	2.8	2.4	3.6	25.5	5.7	3.8	---	---	259
E	3937.0	S	689000	6261676	1.0	6.3	9.6	41.5	9.5	6.2	---	---	0
F	3926.6	S	688998	6261559	3.2	7.4	14.6	46.4	14.5	6.5	0.4	20	0
G	3895.3	S	689002	6261107	2.4	0.0	21.1	17.0	12.8	2.9	---	---	0
H	3812.3	S?	688992	6259287	5.2	31.8	35.9	163.2	30.5	24.2	---	---	0

CX = COAXIAL
CP = COPLANAR

Note:EM values shown above are local amplitudes

*Estimated Depth may be unreliable because the stronger part of the conductor may be deeper or to one side of the flight line, or because of a shallow dip or magnetite/overburden effects

Anomalies Summary

Conductor Grade	No, of Responses
7	0
6	0
5	0
4	3
3	4
2	32
1	42
0	329
Total	410

Conductor Model	No, of Responses
B	11
D	1
S	398
Total	410

STATEMENT OF QUALIFICATIONS

I, Mark Stephens of 149-455 Apache Court, Mississauga, Ontario, do hereby certify that:

1. I have received a B.Sc. Honours degree in Earth Sciences and Mathematics from York University in 1989.

2. I have received an M.Sc. degree in Sedimentaology from the University of Toronto in 1992.

3. I have continuously practiced my profession as a geophysicist since 1993 working in Canada, U.S.A., South Africa, Ethiopia, Zimbabwe, Namibia and Cyprus.

4. I have no direct or indirect interest in the properties held by Northgate Exploration.

Dated this day August 28, 2003 Mississauga, Ontario.

Mark Stephens


KLI NO.27
245,158
KLI NO.28
245,159
KC 1
238,258
KC 2
238,259
CROY #12
244,997
CROY #11
244,996
CROY #10
244,995
CROY #9
244,994
CROY #8
244,993
CROY #7
244,992
CROY #6
244,991
CROY #5
244,990
CROY #4
244,989
CROY #3
244,988
CROY #2
244,987
CROY #1
244,986
CROY 1
395,008
CROY 2
CROY 2
395,009
SOUP 12
238,688
SOUP #2
244,015
SOUP #1
244,014
SOUP #4
244,017
SOUP #3
SOUP #6
244,019
SOUP 11 FR.
238,499
SOUP #5
244,018
SOUP #8
244,021
SOUP #7
244,020
SOUP #10
244,023
SOUP #9
244,022
SOUP 15
349,166
SOUP 13
238,689
SOUP 16
350,782,780
SOUP 17
350,783 350,781
CROY 3
395,010
CROY 4
CROY 4
395,011
HEATHER 1
395,437
HEATHER 2
395,438
HEATHER 3
395,439
HEATHER 4
395,440
HEATHER 5
395,441
GRANITE
242,792
BASIN - 3
321,856
CROY 5
395,292
6,267,000
6,266,000
6,265,000
6,264,000
6,263,000
6,262,000
6,261,000
6,260,000
6,259,000
6,258,000
6,257,000
6,256,000
678,000
679,000
680,000
681,000
682,000
683,000
684,000
685,000
686,000
687,000
688,000
689,000
690,000
691,000
692,000
693,000
0
1.5
3
kilometers
Northgate Exploration Limited
Croy Property – Claims
Scale = 1:20000

M2

TECHNICAL SUMMARY

Navigation	Differentially-corrected GPS
Data reduction grid interval	50 metres
Terrain clearance	Helicopter, Spectrometer 57 m Electromagnetic sensor 30 m Magnetometer 30 m
Data sampling interval	0.1 second
Magnetometer / sensitivity	Cesium / 0.01 nT
Electromagnetic system	DIGHEM^V
Spectrometer	GR820

Frequency	Sensitivity	Coil Orientation
1000 Hz	.06 ppm	Vertical coaxial
5500 Hz	.12 ppm	Vertical coaxial
900 Hz	.12 ppm	Horizontal coplanar
7200 Hz	.24 ppm	Horizontal coplanar
56000 Hz	.60 ppm	Horizontal coplanar

ELECTROMAGNETIC ANOMALIES

Grade	Anomaly	Conductance
7	●	>100 siemens
6	◕	50–100 siemens
5	◑	20–50 siemens
4	◔	10–20 siemens
3	⊕	5–10 siemens
2	○	1–5 siemens
1	◌	< 1 siemens
–	✳	Questionable anomaly

Anomaly identifier → Interpretive symbol (e.g. C|H)

Depth is greater than
- . 15 m
- : 30 m
- ⁞ 45 m
- ⁞. 60 m

Inphase and Quadrature of coaxial coil is greater than
- . 5 ppm
- .. 10 ppm
- ... 15 ppm
- .... 20 ppm

Interpretive symbol	Conductor ("model")
B	Bedrock conductor
D	Narrow bedrock conductor ("thin dike")
S	Conductive cover ("horizontal thin sheet")
H	Broad conductive rock unit, deep conductive weathering, thick conductive cover ("half space")
E	Edge of broad conductor ("edge of half space")
L	Culture, e.g. power line, metal building or fence

FLIGHT LINES WITH EM ANOMALIES

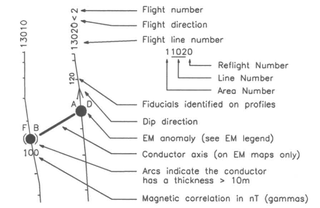

TOTAL MAGNETIC FIELD CONTOURS

- ——— . . . . . 250 nT
- ——— . . . . . 50 nT
- ——— . . . . . 10 nT
- — — — — . . . . . 5 nT
- ⬭ . . . . . magnetic low

Magnetic inclination within the survey area: 75 degrees N
Magnetic declination within the survey area: 23 degrees E

LOCATION MAP

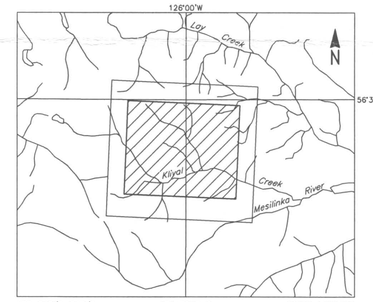

NTS: 94C/5; 94D/8 UTM ZONE: 9 NAD27 SCALE: 1:250,000

NORTHGATE EXPLORATION LIMITED
CROY PROPERTY, KLIYUL CREEK, B.C.

TOTAL MAGNETIC FIELD

FUGRO DIGHEM^V SURVEY	NTS: 94C/5; 94D/8	GEOPHYSICIST:
DATE: AUGUST, 2002	JOB: 2116	SHEET: 1

Fugro Airborne Surveys

0 1 2 Km
0 1 Mi
Scale 1:20 000

FUGRO AIRBORNE SURVEYS

M3

TECHNICAL SUMMARY

Navigation	Differentially-corrected GPS
Data reduction grid interval	50 metres
Terrain clearance	Helicopter, Spectrometer 57 m Electromagnetic sensor 30 m Magnetometer 30 m
Data sampling interval	0.1 second
Magnetometer / sensitivity	Cesium / 0.01 nT
Electromagnetic system	DIGHEM^V
Spectrometer	GR820

Frequency	Sensitivity	Coil Orientation
1000 Hz	.06 ppm	Vertical coaxial
5500 Hz	.12 ppm	Vertical coaxial
900 Hz	.12 ppm	Horizontal coplanar
7200 Hz	.24 ppm	Horizontal coplanar
56000 Hz	.60 ppm	Horizontal coplanar

ELECTROMAGNETIC ANOMALIES

Grade	Anomaly	Conductance
7	●	>100 siemens
6	◕	50-100 siemens
5	◑	20-50 siemens
4	◔	10-20 siemens
3	⊕	1-5 siemens
2	○	< 1 siemens
–	✳	Questionable anomaly

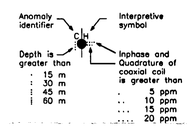

Interpretive symbol	Conductor ("model")
B	Bedrock conductor
D	Narrow bedrock conductor ("thin dike")
S	Conductive cover ("horizontal thin sheet")
H	Broad conductive rock unit, deep conductive weathering, thick conductive cover ("half space")
E	Edge of broad conductor ("edge of half space")
L	Culture, e.g. power line, metal building or fence

FLIGHT LINES WITH EM ANOMALIES

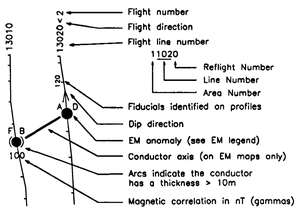

RESISTIVITY CONTOURS

1000
800
600
500
400
300
250
200
150
125
100

Contours in ohm-m at 10 intervals per decade.
Apparent resistivity calculated using a pseudo-layer half-space model (Fraser 1978).

LOCATION MAP

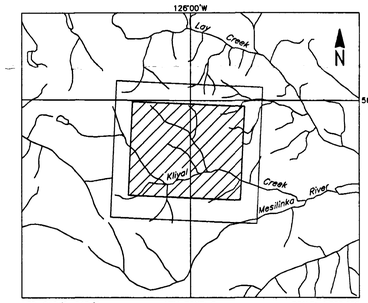

NTS: 94C/5; 94D/8 UTM ZONE: 9 NAD27 SCALE: 1:250,000

NORTHGATE EXPLORATION LIMITED
CROY PROPERTY, KLIYUL CREEK, B.C.

APPARENT RESISTIVITY
900 Hz COPLANAR

FUGRO DIGHEM^V SURVEY	NTS: 94C/5; 94D/8	GEOPHYSICIST:
DATE: AUGUST, 2002	JOB: 2116	SHEET: 1

Fugro Airborne Surveys

0 1 2 Km
0 1 Mi
Scale 1:20 000

FUGRO AIRBORNE SURVEYS

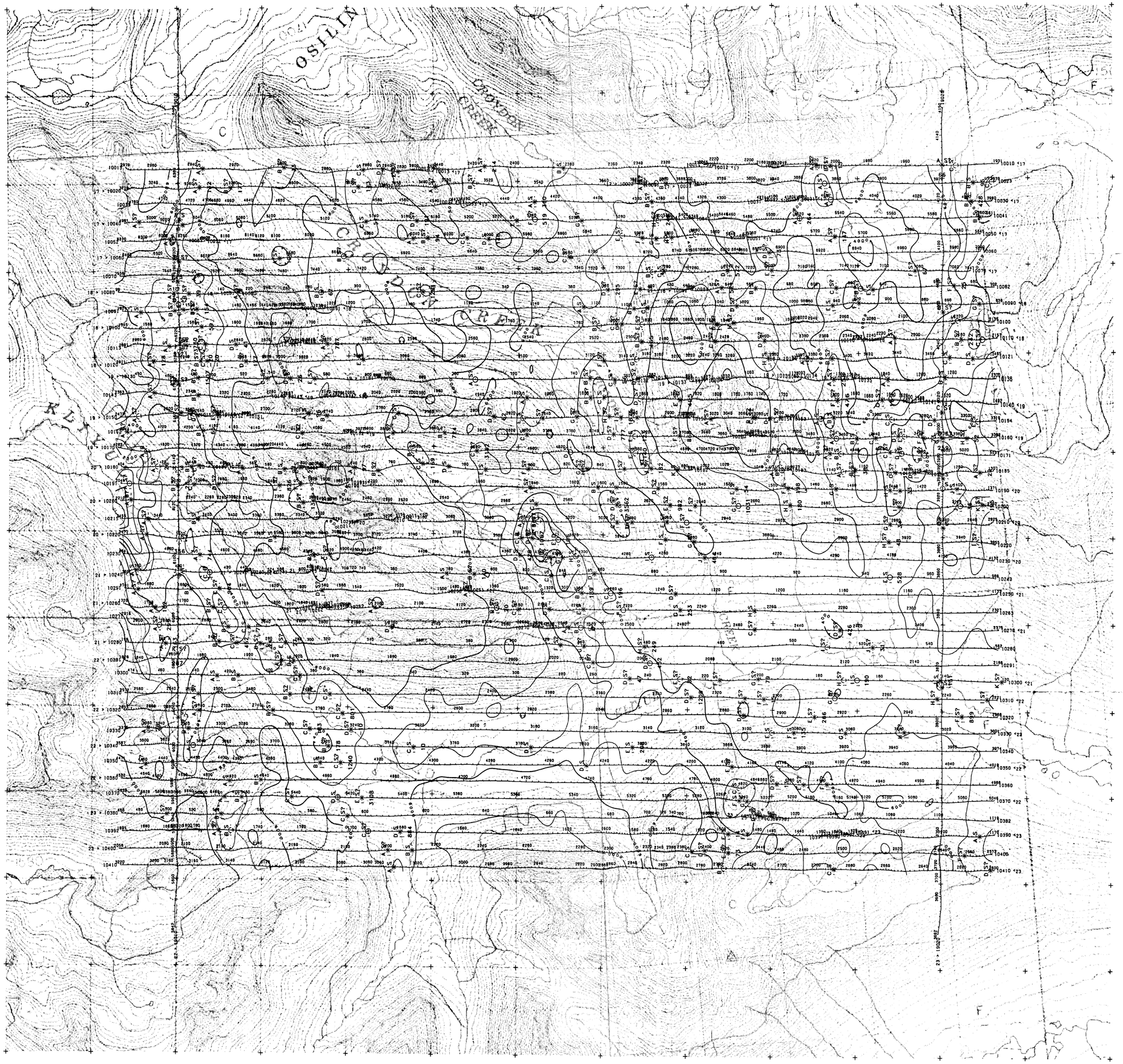

TECHNICAL SUMMARY

Navigation	Differentially-corrected GPS
Data reduction grid interval	50 metres
Terrain clearance	Helicopter, Spectrometer 57 m Electromagnetic sensor 30 m Magnetometer 30 m
Data sampling interval	0.1 second
Magnetometer / sensitivity	Cesium / 0.01 nT
Electromagnetic system	DIGHEM^V
Spectrometer	GR820

Frequency	Sensitivity	Coil Orientation
1000 Hz	.06 ppm	Vertical coaxial
5500 Hz	.12 ppm	Vertical coaxial
900 Hz	.12 ppm	Horizontal coplanar
7200 Hz	.24 ppm	Horizontal coplanar
56000 Hz	.60 ppm	Horizontal coplanar

ELECTROMAGNETIC ANOMALIES

Grade	Anomaly	Conductance
7	●	>100 siemens
6	◕	50–100 siemens
5	◑	20–50 siemens
4	◔	10–20 siemens
3	⊕	5–10 siemens
2	○	1–5 siemens
1	◌	< 1 siemens
–	✳	Questionable anomaly

Anomaly identifier — Interpretive symbol — Depth is greater than: . 15 m, : 30 m, ⁝ 45 m, ⁞ 60 m — Inphase and Quadrature of coaxial coil is greater than: . 5 ppm, .. 10 ppm, ... 15 ppm, ... 20 ppm

Interpretive symbol	Conductor ("model")
B	Bedrock conductor
D	Narrow bedrock conductor ("thin dike")
S	Conductive cover ("horizontal thin sheet")
H	Broad conductive rock unit, deep conductive weathering, thick conductive cover ("half space")
E	Edge of broad conductor ("edge of half space")
L	Culture, e.g. power line, metal building or fence

FLIGHT LINES WITH EM ANOMALIES

13010 — 13020-2 — 120 — 11020 (Reflight Number / Line Number / Area Number) — A — D — F B — 100

- Flight number
- Flight direction
- Flight line number
- Fiducials identified on profiles
- Dip direction
- EM anomaly (see EM legend)
- Conductor axis (on EM maps only)
- Arcs indicate the conductor has a thickness > 10m
- Magnetic correlation in nT (gammas)

RESISTIVITY CONTOURS

1000 — 800 — 600 — 500 — 400 — 300 — 250 — 200 — 150 — 125 — 100

Contours in ohm-m at 10 intervals per decade. Apparent resistivity calculated using a pseudo-layer half-space model (Fraser 1978).

LOCATION MAP

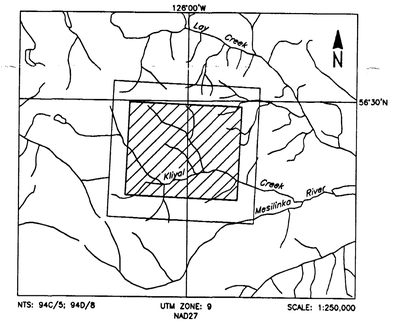

NTS: 94C/5; 94D/8 — UTM ZONE: 9 NAD27 — SCALE: 1:250,000

NORTHGATE EXPLORATION LIMITED
CROY PROPERTY, KLIYUL CREEK, B.C.

APPARENT RESISTIVITY
7200 Hz COPLANAR

FUGRO DIGHEM^V SURVEY	NTS: 94C/5; 94D/8	GEOPHYSICIST:
DATE: AUGUST, 2002	JOB: 2116	SHEET: 1
Fugro Airborne Surveys		

0 — 1 — 2 Km
0 — 1 MI
Scale 1:20 000

FUGRO AIRBORNE SURVEYS